A New Simple Approach for Constructing Implied Volatility Surfaces

Peter Carr[*]

Courant Institute, New York University

Liuren Wu[†]

Zicklin School of Business, Baruch College, The City University of New York

This version: October 2, 2010; First draft: September 27, 2009

Abstract

Standard option pricing models specify the dynamics of the security price and the instantaneous variance rate, and derives its no-arbitrage implication for the option implied volatility surface. Market models start with an initial implied volatility surface and a diffusion specification for the implied volatility dynamics, and derive the no-arbitrage constraints on the risk-neutral drift of the dynamics. This paper proposes a new approach, which specifies the security price and the implied volatility dynamics while leaving the instantaneous variance rate dynamics unspecified. The allowable shape for the initial implied volatility surface is then derived based on dynamic no-arbitrage arguments. Two parametric specifications for the implied volatility dynamics lead to extreme tractability, as the whole implied volatility surface is determined by a quadratic equation. The paper also proposes a dynamic calibration methodology and calibrates the two models to over-the-counter currency option and equity index option implied volatility surfaces over an 11-year period. The model with lognormal implied variance dynamics generates superior performance over standard option pricing models of similar complexities. Furthermore, constructing implied volatility surfaces using our two models is 100 times faster than using traditional option pricing models.

JEL Classification: C13, C51, G12, G13.

Keywords: Implied volatility surface; vega-gamma-vanna-volga; square-root variance model; lognormal variance model; dynamic calibration; unscented Kalman filter.

We thank Bruno Dupire, Robert Engle, Travis Fisher, Rachid Lassoued, Alex Levin, Keith Lewis, Dilip Madan, Fabio Mercurio, Attilio Meucci, Alexey Polishchuk, Jason Roth, Arun Verma, and seminar participants at Baruch College and the Fields Institute for their comments and suggestions. We welcome comments, including references that we have inadvertently missed.

[*]251 Mercer Street, New York, NY 10012; (212) 507-2636; pcarr@nyc.rr.com.

[†]One Bernard Baruch Way, Box B10-225, New York, NY 10010; (646) 312-3509; liuren.wu@baruch.cuny.edu.

Contents

There is widespread agreement that the geometric Brownian motion dynamics used by Black and Scholes (1973) and Merton (1973) to price options is too restrictive. Nonetheless, practitioners commonly use the Black-Merton-Scholes (BMS) implied volatilities as a communication tool. Academics also frequently rely on the variations of implied volatilities across option strike prices, maturities, and calendar time to infer how the underlying security price dynamics deviate from the BMS assumption. For example, when the implied volatilities are plotted against the strike price at a fixed maturity, one often observes a skew or smile pattern, which has been shown to be directly related to the conditional non-normality of the underlying return risk-neutral distribution. In particular, a smile reflects fat tails in the return distribution whereas a skew indicates return distribution asymmetry. Furthermore, how the implied volatility smile varies across option maturity and calendar time reveals how the conditional return distribution non-normality varies across different conditioning horizons and over different time periods.

The literature takes two distinct approaches in capturing the deviations from the original BMS model assumptions. The academic literature often starts by assuming a security price dynamics that can accommodate the observed implied volatility smiles and skews, as well as their variations. For example, various Lévy jump processes have been proposed to capture smiles at short maturities.[1] Stochastic volatility models have been proposed to capture the implied volatility smiles at intermediate maturities as well as time variations in the implied volatility levels.[2] Jumps and stochastic volatilities have also been combined in various forms to capture implied volatility behaviors over different strikes, maturities, and calendar days.[3] The general procedure for this strand of literature is to first propose a security price dynamics, and then estimate the coefficients of the dynamics on observed option prices, either through static daily calibration or through a dynami-

[1] Prominent examples include Merton (1976), Barndorff-Nielsen (1998), Madan, Carr, and Chang (1998), Eberlein, Keller, and Prause (1998), Carr, Geman, Madan, and Yor (2002), Kou (2002), Carr and Wu (2003), Schoutens (2003), and Wu (2006).

[2] See, for example, Heston (1993) and Hull and White (1987)

[3] Examples include Bates (1996), Bakshi, Cao, and Chen (1997), Carr and Wu (2004, 2007, 2008, 2010), Huang and Wu (2004), and Bakshi, Carr, and Wu (2008).

cally consistent estimation procedure that fix the model parameters while allowing the stochastic quantities to vary over time. The estimated model yields a smooth, but usually imperfect, fitting of the observed option prices. The performance of such a model can be judged by the size and property of the fitting error. From a market maker's perspective, the pricing errors should be small and preferably within the bid-ask band as a market maker can rarely take views against the whole market. From an investor's perspective, the pricing errors can be large, but they must be highly transient so that trades based on the pricing errors can converge quickly. In both cases, a good model should capture the underlying risk sources accurately so that hedging based on the model can truly eliminate risk exposures.

Practitioners' heavy reliance on implied volatilities has also spurred another strand of literature that starts directly with a dynamic specification of the implied volatility themselves. These models are often called *market models* of implied volatility. In general, this approach begins by assuming that the entire implied volatility surface has known initial value and evolves continuously over time. The approach first specifies the continuous martingale component of the volatility surface, and then derives the restriction on the risk-neutral drift of the surface imposed by the requirement that all discounted asset prices be martingales.[4] Once the model is calibrated, one can hedge the given vanilla options, and price and hedge all contingent claims written on the paths of the stock and/or implied volatilities.

A common criticism against the market model approach is that the knowledge of the initial implied volatility surface places unclear constraints on the specification of the continuous martingale component of its subsequent dynamics. For example, if at inception, the graph of implied volatility against strike price slopes down at each maturity date, one is likely not able to assume positive correlation between changes in implied volatility and returns from the underlying. If a market maker did nonetheless assume that this correlation is positive, when in fact it is always negative, the con-

[4]Examples include Avellaneda and Zhu (1998), Ledoit and Santa-Clara (1998), Schönbucher (1999), Hafner (2004), Fengler (2005), and Daglish, Hull, and Suo (2007).

cern is that risk reversals will be priced with the wrong sign at future dates, allowing a model-free arbitrage.

This paper proposes a new approach that falls in between the two existing strands of literature. The resultant models from this new approach are much simpler than most models for either approach. Similar to the market model approach, we also directly model the dynamics of implied volatilities. However, instead of taking the initial implied volatility surface as given and infer the risk-neutral drift of the implied volatility dynamics, we specify both the risk-neutral drift and the martingale component of the implied volatility dynamics, from which we *derive* the allowable shape for the implied volatility surface. As such, the shape of the initial implied volatility surface is guaranteed to be consistent with the specified implied volatility dynamics. In this sense, our approach is also similar to the first strand of literature, except that our dynamics are specified on the implied volatilities, rather than on an instantaneous variance rate. Furthermore, we do not take the whole implied volatility surface as given, but rather assume that we only observe a few implied volatilities, with which we calibrate the implied volatility dynamics and then construct the whole implied volatility surface from the calibrated dynamics.

We assume that a single standard Brownian motion drives the whole volatility surface, and that a second partially correlated standard Brownian motion drives the underlying security price dynamics. When we enforce the condition that the discounted prices of options and their underlying are martingales under the risk-neutral measure, we obtain a fundamental partial differential equation (PDE) that governs the shape of the implied volatility surface. This PDE relates the BMS theta of the options linearly to the BMS vega, dollar gamma, dollar vanna, and volga of the options, where all the BMS greeks of an option are defined on the BMS implied volatility of this contract. We refer to this fundamental PDE as the Vega-Gamma-Vanna-Volga (VGVV) methodology, as it links the theta of the options and their four greeks (VGVV). Plugging in the analytical solutions for the BMS greeks, we reduce the PDE into an algebraic relation that links the shape of the implied

volatility surface to its risk-neutral dynamics.

By parameterizing the implied variance dynamics as a mean-reverting square-root process, the algebraic equation simplifies into a quadratic equation of the implied volatility surface as a function of a standardized moneyness measure and time to maturity. The coefficients of the quadratic equation are governed by six coefficients related to the dynamics of the stock price and implied variance. We label this model as the square root variance (SRV) model. Alternatively, if we parameterize the implied variance dynamics as a mean-reverting lognormal process, we obtain another quadratic equation of the implied variance as a function of log strike over spot and time to maturity. The whole implied variance surface is again determined by six coefficients related to the stock price and implied variance dynamics. We label this model as the lognormal variance (LNV) model. Compared to standard stochastic variance models such as Heston (1993), our two parameterized stochastic implied variance models are much simpler. Computing BMS implied volatilities from the Heston model involves numerical approximations of an integration or Fourier transform, as well as a nonlinear optimization routine to solve for the implied volatility from the option value. By contrast, computing BMS implied volatilities from our two models (SRV and LNV) only involves writing out the solutions to the two quadratic equations.

We propose a dynamic calibration approach for the model coefficients, in which we set up a state-space framework by regarding the model coefficients as the hidden states and regarding the finite number of implied volatility observations as noisy observations. Then, we infer the unobserved states (coefficients) from the implied volatility observations based on the unscented Kalman filter (UKF) of Julier and Uhlmann (1997). The auxiliary parameters that govern the time-variation of the coefficients and the size of the noise in the implied volatility quotes can be estimated via a quasi-likelihood method. Once these auxiliary parameters are estimated, the UKF provides a fast calibration of implied volatility surfaces from implied volatility quotes.

To gauge the empirical performance our two parametric specifications, we calibrate the two

models to both over-the-counter (OTC) currency options and OTC S&P 500 index (SPX) options and compare their performance to that of the Heston model. We analyze currency options on two currency pairs: the dollar-pound and the dollar-yen exchange rate. The options are quoted in terms of fixed time to maturity and fixed BMS delta implied volatilities. These volatilities are often quoted in combinations in terms of straddles, risk reversals, and butterfly spreads to reflect the implied volatility levels, skews, and smiles. The data contain 11 maturities from one month to five years and five deltas at each maturity. We sample the data weekly from January 8, 1997 to December 26, 2007, spanning 573 weeks. Over our sample period, the OTC currency options market has experienced some structural changes. The long-dated risk reversals and butterfly spreads are often set to zero before 2000, but have since been allowed to take large values that vary over time. All three models are capable of capturing the various implied volatility surface shapes on the two currency pairs, with the LNV model performing the best for both currency pairs. Furthermore, calibrating our two models is about 100 times faster than calibrating the Heston model.

The OTC SPX options are quoted in terms of implied volatilities at fixed time to maturities and relative strikes in percentages of the spot level. The data at each date contain eight time to maturities from one month to five years, and five strikes from 80% to 120% of the spot level. The data are for the same sample period as that for the currency options. The implied volatilities on the equity index options are heavily negatively skewed, more so at long maturities than at short maturities. The implied volatility level also tends to be higher at longer maturities, except at crisis times when the short-term implied volatility can spike and the term structure becomes downward sloping. The calibration exercise again identifies the LNV model as the best performing. Compared to the Heston model, the LNV model generates about half the size on the root mean squared pricing errors, explains five percentage points more variation in implied volatilities, and generates pricing errors with 13 percentage points lower serial correlation. On top of all the superior pricing performance, the model can be calibrated 100 times faster.

Our fundamental VGVV PDE builds on the options's greeks under the BMS model. In related literature, Wystup (2008) and Castagna and Mercurio (2007) propose an option valuation method based on the options' BMS vega, vanna, and volga, henceforth the VVV model. Our VGVV model differs from this VVV approach in several ways. First, our VGVV analysis is carried out in implied volatility space, whereas the VVV analysis is carried out in option price space. Second, all the BMS greeks in the VVV approach are evaluated at a reference implied volatility (typically at the money) rather than at each of the four options' own implied volatility. The VVV approach begins by defining a reference implied volatility and then computing a BMS reference option value at each strike based on this single reference implied volatility. Then, the price difference of a target option from its BMS reference value is assumed to be linear in the price difference of three pillar options from their BMS reference values. The three coefficients are determined by equating vega, vanna, and volga of the target option and the portfolio of the three pillar options, with all the greeks evaluated at the reference implied volatility. This method is used as an approximate way to adjust the value of any derivative security by linking its deviation from its BMS reference value linearly to the observed deviations at three pillar points.

Practitioners are deeply entrenched in the BMS implied volatilities, even though the BMS model is clearly violated whenever implied volatilities differ across strike. There are several good reasons for this entrenchment. First, the the implied volatility plot against strikes is much more revealing about the underlying return distribution than a direct plot of the option price against strike. Second, through the use of implied volatilities, one can directly exclude several sources of arbitrage opportunities. In a classic paper, Merton (1973) develops the model-free bounds on option prices arising from no static arbitrage. Hodges (1996) shows that by quoting an option in terms of a positive implied volatility, several no-arbitrage bounds are automatically guaranteed: Call and put prices must never fall below intrinsic value, call prices must never exceed the (dividend discounted) stock price, and put prices must never exceed the (present value of the) strike price.

Furthermore, put-call parity is automatically guaranteed if one positive implied volatility is quoted for the call and put options at the same strike and maturity. These properties make it very attractive for market makers to quote on implied volatilities based on options order flows while letting an automated system to update the option prices automatically whenever the underlying security price moves.

Unfortunately, quoting implied volatilities does not exclude arbitrage of all types. If implied volatility slopes up or down too fast in strike, bull and bear spreads can be priced negatively. If implied volatility slopes down too fast in maturity, calendar spreads can be priced negatively. If implied volatility is too concave in strike, butterfly spreads can be priced negatively. All these lead to arbitrage opportunities between options on the same underlying security. The objective of this paper is to derive no-arbitrage constraints on the shape of the implied volatility surface by assuming dynamics on the implied volatilities.

After the seminal work by BMS on dynamic replication, Cox and Ross (1976) highlight the importance of so-called risk-neutral pricing in Markovian settings. Employing results from the general theory of stochastic processes, Harrison and Kreps (1979) and Harrison and Pliska (1981) develop this insight into the martingale restriction on relative asset prices arising from no dynamic arbitrage. In this paper, we consider the effect of these martingale restrictions on the shape of implied volatility surfaces in a simplified setting. By specifying the dynamics of the stock price and all implied volatilities in a continuous manner, we find a simple condition that can be used to develop the entire implied volatility surface from knowledge of a few known points.

The remainder of the paper is organized as follows. Section 1 establishes our theoretical framework by specifying implied volatility dynamics and deriving the allowed shapes for the implied volatility surfaces. Section 2 proposes a dynamic approach for fast calibration of the implied volatility surface to the implied volatility dynamics. Section 3 discusses the results from calibrating OTC currency option implied volatility surfaces on two currency pairs: the dollar price of yen

and the dollar price of pound. Section 4 discusses the results from calibrating the OTC S&P 500 index option implied volatility surfaces. Section 5 provides concluding remarks and directions for future research.

1. From Implied Volatility Dynamics to Surfaces

1.1. Assumptions and notations

We initially consider a market with a riskless asset, a risky asset, and an option written on the risky asset. We will later introduce a finite number of additional options. For simplicity, we assume zero interest rates and that the underlying has no carrying costs. While the underlying can be any asset that can be traded continuously, we will refer to it as the stock. We allow frictionless and continuous trading in the riskfree asset, the stock, and the one option. When other options are introduced, they need only be held static. The set of events which can and cannot occur is assumed known, but the likelihood of events under the statistical probability measure $\mathbb{P}$ need not be known. We assume no arbitrage between the stock and the riskless asset. As a result, there exists a risk-neutral probability measure $\mathbb{Q}$, equivalent to $\mathbb{P}$, such that the stock price S is a martingale.

We assume that the underlying stock price S evolves in continuous time as a strictly positive and continuous semi-martingale. By the martingale representation theorem, there exists a standard Brownian motion W under $\mathbb{Q}$ such that the stock price S solves the following stochastic differential equation:

$$dS_t/S_t = s_t dW_t, \quad t \geq 0, \tag{1}$$

where the initial stock price is assumed known and s_t denote the time-t instantaneous return volatility of the stock at time t. We allow s to follow a real-valued stochastic process such that there exists a unique solution to (1). However, in contrast to most of the stochastic volatility literature, we do

not directly specify the risk-neutral dynamics of this process. Instead, we will specify the risk-neutral dynamics of each option's implied volatility.

We assume that each option's implied volatility $I(K,T)$ is a continuous semi-martingale and a solution of the following stochastic differential equation under the risk-neutral probability measure $\mathbb{Q}$:

$$dI_t(K,T) = \mu_t dt + \omega_t dZ_t, \quad t \geq 0 \tag{2}$$

for all $K > 0$ and $T > t$. We refer to μ as the drift process and ω as the volatility of volatility process (henceforth "volvol" for short). Both processes can be stochastic and they can both depend on deterministic quantities such as calendar time t, strike price K, and maturity date T. In contrast to μ and ω, the standard Brownian motion Z is independent of the strike K and maturity T at all times. In essence, equation (2) assumes that instantaneously, the whole implied volatility surface is driven by one Brownian shock. We allow correlation between the the stock price and the implied volatilities,

$$d\langle W, Z\rangle_t = \rho_t dt, \quad t \in [0,T], \tag{3}$$

where ρ_t is a stochastic process taking values in the interval $[-1,1]$.

In market models of implied volatility, one takes the initial implied volatility surface as a known function, and specifies the volvol process ω_t. Then, the presumed absence of no dynamic arbitrage is used as the guiding principle to determine the risk-neutral drift μ_t of each point on the implied vol surface. By contrast, in this paper we specify both the risk-neutral drift μ_t and the volvol process ω_t, and explore the implications of these specifications on the shape of the initial implied volatility surface.

1.2. The fundamental PDE governing the implied volatility surface

Let $P_t(K,T)$ denote the European put option price at strike K and maturity T. We use the put option for concreteness. The same argument can go through for call options as well. Let $B(S,\sigma,t;K,T)$: $\mathbb{R}^+ \times \mathbb{R}^+ \times [0,T) \mapsto \mathbb{R}^+$ be the BMS model formula for the value of this European put option:

$$B(S,\sigma,t;K,T) \equiv KN(z(S,\sigma,t)) - SN(z(S,\sigma,t) - \sigma\sqrt{T-t}), \tag{4}$$

where the real-valued function

$$z(S,\sigma,t;K,T) \equiv \frac{\ln(K/S)}{\sigma\sqrt{T-t}} + \frac{\sigma\sqrt{T-t}}{2}, \tag{5}$$

is a standard σ-dependent measure of the moneyness of the put. For brevity, we henceforth suppress the notational dependence of B and z on K and T.

By the definition of implied volatility, we have

$$P_t(K,T) = B(S_t, I_t(K,T), t), \tag{6}$$

for all $t \geq 0$, $K > 0$, and $T > t$. It is well known that the function $B(S,\sigma,t)$ is $C^{2,2,1}$ on $\mathbb{R}^+ \times \mathbb{R}^+ \times [0,T)$, so Itô's formula can be used to relate increments of P to the increments of S, I, and t. To shorten the length of the following equations, we let subscripts of B denote partial derivatives and we suppress the arguments of B, which are always $(S_t, I_t(K,T), t)$. The following theorem links the functions $B(S,\sigma,t)$ and $I_t(K,T)$ through a fundamental partial differential equation (PDE), which is derived based on the principle of no dynamic arbitrage.

Theorem 1 *Under the diffusion stock price dynamics in (1), the diffusion implied volatility dynamics in (2), and the correlation specification in (3), the absence of dynamic arbitrage on an*

option contract $P_t(K,T)$ dictates that the BMS option pricing function $B(S,\sigma,t)$ and the implied volatility function $I_t(K,T)$ for this option jointly solve the following fundamental PDE:

$$-B_t = \mu_t B_\sigma + \frac{s_t^2}{2} S_t^2 B_{SS} + \rho_t \omega_t s_t S_t B_{S\sigma} + \frac{\omega_t^2}{2} B_{\sigma\sigma}. \tag{7}$$

Proof. Applying Ito's lemma on BMS function in equation (6) yields,

$$\begin{aligned} dP_t(K,T) &= B_S dS_t + B_\sigma dI_t(K,T) + B_t dt \\ &\quad + \frac{1}{2} B_{SS} d\langle S\rangle_t + B_{S\sigma} d\langle S, I(K,T)\rangle_t + \frac{1}{2} B_{\sigma\sigma} d\langle I(K,T)\rangle_t. \end{aligned} \tag{8}$$

From (1), (2), and (3), we can write the quadratic variation terms as

$$d\langle S\rangle_t = S_t^2 s_t^2 dt, \quad d\langle S, I\rangle_t = s_t \omega_t \rho_t S_t dt, \quad d\langle I(K,T)\rangle_t = \omega_t^2 dt, \quad t \geq 0. \tag{9}$$

Substituting (1), (2), and (9) in (8) implies

$$dP_t(K,T) - B_S s_t S_t dW_t - B_\sigma \omega_t dZ_t = [\mu_t B_\sigma + B_t + \frac{S_t^2 s_t^2}{2} B_{SS} + \rho_t \omega_t s_t S_t B_{S\sigma} + \frac{\omega_t^2}{2} B_{\sigma\sigma}] dt. \tag{10}$$

The absence of dynamic arbitrage implies that there exists a measure $\mathbb{Q}$ under which $P(K,T)$, W, and Z are all martingales. Taking conditional expectations on both sides of (10) under $\mathbb{Q}$ leads to the partial differential equation in (7). ■

The terminology used to describe the various terms involving partial derivatives of B in fundamental PDE in (7) are theta for B_t, vega for B_σ, dollar gamma for $S_t^2 B_{SS}$, dollar vanna for $S_t B_{S\sigma}$, and volga for $B_{\sigma\sigma}$. Thus, equation (7) defines a linear relation between the theta of the option and its vega, dollar gamma, dollar vanna, and volga. We christen the class of implied volatility surfaces defined by the fundamental PDE in (7) as the **Vega-Gamma-Vanna-Volga (VGVV)** model.

While equation (7) is developed for European options, it also applies for any fixed σ in any region of (S,t) where the BMS PDE is valid and whenever the BMS value function is increasing in σ. Hence, (7) also applies to American options in the continuation region. Once the coefficients in equation (7) are known, lattices, trees, grids, Monte Carlo and other numerical methods can be employed for these options.

By plugging in the partial derivatives of the BMS option pricing function, we can reduce the PDE into an algebraic equation that links the future implied volatility dynamics to its current shape.

Proposition 1 *Under dynamic no arbitrage, the current implied volatility surface $I_t(K,T)$ is fully determined by the current instantaneous return volatility level s_t, the implied volatility dynamics (μ_t,ω_t) and the instantaneous correlation between return and implied volatility (ρ_t) through the following algebraic equation,*

$$\begin{aligned}&\frac{I_t^2(K,T)}{2}-\mu_t I_t(K,T)(T-t)-\frac{s_t^2}{2}-\rho_t\omega_t s_t z(S_t,I_t(K,T),t)\sqrt{T-t}\\&-\frac{\omega_t^2}{2}[z^2(S_t,I_t(K,T),t)-I_t(K,T)\sqrt{T-t}z(S_t,I_t(K,T),t)](T-t)=0.\end{aligned}\tag{11}$$

Proof. It is the property of the BMS European put formula that:

$$\begin{aligned}&B_t=-\tfrac{\sigma^2}{2}S^2B_{SS}, && B_\sigma=\sigma(T-t)S^2B_{SS},\\&SB_{\sigma S}=z(S,\sigma,t)\sqrt{T-t}S^2B_{SS}, && B_{\sigma\sigma}=[z^2(S,\sigma,t)-\sigma\sqrt{T-t}z(S,\sigma,t)](T-t)S^2B_{SS}\end{aligned}\tag{12}$$

Evaluating these results at $(S,\sigma,t)=(S_t,I_t(K,T),t)$, substituting them into (7), dividing both sides of the equation by the dollar gamma $S_t^2B_{SS}$ while noting that the dollar gamma is strictly positive at $T>t$, we obtain equation (11). ■

Just as integral transforms often convert partial differential equations into algebraic equations,

the use of implied volatility has transformed the second order parabolic PDE in (7) into the simple algebraic relation (11). Under our dynamic assumptions for the stock price and the implied volatilities in (1) to (3), a necessary condition arising from no arbitrage is that the current implied volatility surface $I_t(K,T)$ resides in the manifold defined by (11).

By assuming a zero drift on the implied volatility dynamics, and further assuming that the volvol process ω_t is independent of K and $I_t(K,T_0)$, Arslan, Eid, Khoury, and Roth (2009) derives a special case of equation (7) that involves only gamma, vanna, and volga of the option, but not the option's vega. They label their model as the GVV model and use it for calibration the implied volatility smile at one maturity.

In practice, there is no compelling reason to treat each maturity separately. Furthermore, this single maturity focus makes identification of any non-zero risk-neutral drift μ numerically difficult, even if it is theoretically possible. In contrast, we show that it is quite feasible to identify risk-neutral drift and all of the other state variables when calibrating simultaneously to options of multiple maturities and strikes. In what follows, we consider two representations of the implied volatility surface, one in terms of a normalized moneyness measure and time to maturity (term) and the other in terms of log strike relative to spot and term. In each case, we propose a particular implied volatility dynamics that yields an extremely tractable functional form for the implied volatility surface.

1.3. Implied volatility as a function of standardized moneyness and term

The literature often characterizes the implied volatility surface in terms of time to maturity (or term) $\tau \equiv T-t$ instead of the maturity date T, and in terms of a standardized moneyness measure such as z defined in (5) instead of the strike price,[5] with the implied volatility replacing the σ in

[5] See discussions in, for example, Backus, Foresi, and Wu (1997), Carr and Wu (2003), and Foresi and Wu (2005).

the definition,

$$z_t \equiv z(S_t, I_t(K,T), t). \tag{13}$$

This moneyness measure can be written as,

$$z_t = \frac{\ln(K) - \left[\ln S_t - \frac{I_t^2(K,T)(T-t)}{2}\right]}{I_t(K,T)\sqrt{\tau}}. \tag{14}$$

If we use $\mathbb{B}(K,T)$ to denote the probability measure that arises in the BMS model when $I_t(K,T)$ is the constant volatility over (t,T), we have the mean and standard deviation of the log stock price as,

$$\mathbb{E}_t^{\mathbb{B}(K,T)} \ln S_T \equiv \ln S_t - \frac{I_t^2(K,T)\tau}{2} \text{ and } \text{Std}_t^{\mathbb{B}(K,T)} \ln S_T \equiv I_t(K,T)\sqrt{\tau}. \tag{15}$$

Substituting (15) in (14) implies that

$$z_t = \frac{\ln(K) - \mathbb{E}_t^{\mathbb{B}(K,T)} \ln S_T}{\text{Std}_t^{\mathbb{B}(K,T)} \ln S_T}. \tag{16}$$

Hence, z_t can be interpreted as the number of standard deviations, $\text{Std}_t^{\mathbb{B}} \ln S_T$, by which the log strike, $\ln(K)$, exceeds the mean of the terminal log price, $\mathbb{E}_t^{\mathbb{B}} \ln S_T$, in the BMS model for which $I_t(K,T)$ is the constant volatility over (t,T).

Let $v_t(z,\tau)$ denote the implied volatility surface as a function of the standardized moneyness measure z and the time to maturity τ,

$$v_t(z,\tau) \equiv I_t(K,T). \tag{17}$$

The following proposition represents the volatility surface $v_t(z,\tau)$ in a new algebraic equation.

Proposition 2 *When the implied volatility surface is represented in terms of the standardized mon-*

eyness z and the time to maturity τ *as in (17), the algebraic equation for* $v_t(z,\tau)$ *becomes,*

$$\frac{v_t^2(z,\tau)}{2} - [\mu_t\tau - \frac{\omega_t^2}{2}z\tau^{\frac{3}{2}}]v_t(z,\tau) - \left[\frac{s_t^2}{2} + \rho_t\omega_t s_t z\sqrt{\tau} + \frac{\omega_t^2}{2}\tau z^2\right] = 0. \tag{18}$$

Equation (18) can be directly obtained from equation (11) via change of variables. The relation imposes a strong restriction on the behavior of implied volatility surface at short maturities. Assume that the processes μ_t and ω_t both stay finite as each option nears expiry, setting $\tau = 0$ in (18) implies that the smile in z becomes flat as the option's term shrinks to zero:

$$\lim_{\tau\downarrow 0} v_t(z,\tau) = s_t, \tag{19}$$

for all z. This result is due to the assumption of no jumps in the stock price dynamics in (1). The limiting behavior in (19) would still hold had we allowed jumps in s and I. All models with continuous stock price dynamics behave alike at short horizons. If the market displays alternative behavior, one can either rely on continuity and exploit the arbitrage or change the model to accommodate the observed behavior. Possible modeling solutions in a continuous time setting include adding jumps in S or assuming that the instantaneous volatility s_t can only be observed with noise at time t.

Equation (18) reflects a simple intuition for the at-the-money volatility $a_t(\tau) \equiv v_t(0,\tau)$. Setting $z = 0$ in (18) implies that:

$$\frac{a_t^2(\tau)}{2} - \mu_t\tau a_t(\tau) = \frac{s_t^2}{2}. \tag{20}$$

Hence, the at-the-money term structure is unaffected by the choice of the volvol process ω nor by the choice of the correlation process ρ_t. At each term τ, $z = 0$ is the only moneyness level where this independence to ω and ρ arises.

When z is defined as the moneyness variable, the initial instantaneous volatility level s_t and the

specification of the implied volatility drift process μ determine the at-the-money implied volatility term structure. The specification of the volvol process ω determines the remainder of the implied volatility surface. As a result, a market maker or risk-manager who only needs the at-the-money term structure does not need to model the volvol process.

Conversely, if we are willing to assume that the implied volatility path is a random differentiable function of time and as such $\omega = 0$, μ_t and s must then both reduce to deterministic functions of time to exclude arbitrage. Furthermore, setting $\omega = 0$ in (18) and enforcing determinism on μ_t and s_t implies that v_t is independent of z. In this case, the implied volatility can have different term structure shapes, but its plot against moneyness is always flat.

In general, the processes μ and ω can depend on v and hence it is premature to treat equation (18) as a quadratic function of v. However, by specifying particular parametric functional forms for μ and ω, one can determine the algebraic nature of the manifold (18) in which v resides. The simplest specification for μ and ω is to assume that they are both constant with respect to I. Since s and ρ are already independent of I, equation (18) becomes quadratic in $v(z,\tau)$ and the quadratic root formula implies that v_t is a hyperbola which is asymptotically linear in z. Unfortunately, Rogers and Tehranchi (2010) show that if the processes μ and ω are assumed to be constant with respect to K, T, and I, there is arbitrage in the original dynamic specification (2) of implied volatilities. The arbitrage identified by Rogers and Tehranchi can be excluded if the drift and/or the volvol process depend on I.

We propose a mean-reverting dynamics for the implied variance $I_t^2(K,T)$ with deterministic square-root volatility,

$$dI_t^2(K,T) = \kappa_t[\theta_t - I_t^2(K,T)]dt + 2w_t e^{-\eta_t(T-t}I_t(K,T)dZ_t, \tag{21}$$

where κ, θ, w, and η are nonnegative stochastic processes that do not depend on K, T, or $I(K,T)$.

We furthermore assume that η is strictly positive and hence $\lim_{T\uparrow\infty} e^{-\eta_t(T-t)} = 0$ for each $t \geq 0$. This assumption allows stationarity and capture the commonly observed behavior that the variation of implied volatilities are lower for longer-dated options. The following proposition shows that under this square-root dynamics, equation (18) is quadratic in v.

Proposition 3 *Under the stock price dynamics in (1)-(3), when the implied variance follows the mean-reverting square-root dynamics in (21), the implied volatility surface satisfies the following quadratic relation,*

$$\begin{aligned}&\left(1+\kappa_t\tau\right)v_t^2\left(z,\tau\right)+\left(w_t^2e^{-2\eta_t\tau}\tau^{3/2}z\right)v_t\left(z,\tau\right)\\&-\left[\left(\kappa_t\theta_t-w_t^2e^{-2\eta_t\tau}\right)\tau+s_t^2+2\rho_tw_ts_te^{-\eta_t\tau}\sqrt{\tau}z+w_t^2e^{-2\eta_t\tau}\tau z^2\right]=0.\end{aligned}\tag{22}$$

Proof. Applying Ito's lemma on (21), we obtain the dynamics on the implied volatility as,

$$dI_t(K,T)=\frac{1}{2}\left(\frac{\kappa_t\theta-w_t^2e^{-2\eta_t(T-t)}}{I_t(K,T)}-\kappa_tI_t(K,T)\right)dt+w_te^{-\eta_t(T-t)}dZ_t.\tag{23}$$

Hence, we have

$$\mu_t=\frac{1}{2}\left(\frac{\kappa_t\theta_t-w_t^2e^{-2\eta_t(T-t)}}{I_t(K,T)}-\kappa_tI_t(K,T)\right),\quad\omega_t=w_te^{-\eta_t(T-t)}.\tag{24}$$

Plug (24) into (18) and rearrange, we obtain the implied volatility relation in (22). ■

Given the coefficients $(\kappa_t, w_t, \eta_t, \theta_t, s_t, \rho_t)$, we can solve the whole implied volatility surface analytically as a solution to the quadratic equation in (22). The quadratic equation has two roots, and one of them is negative. We take the positive root as the solution for the implied volatility surface. We label this class of implied volatility surfaces as the **square-root variance (SRV)** model.

In the limit of $\tau = 0$, $v_t(z,0) = s_t$ for all z, satisfying the no-arbitrage requirement. On the

other side of the maturity spectrum, as $\tau \uparrow \infty$, $\lim_{\tau\uparrow\infty} v_t(z,\tau) = \theta$ for all z as long as η is strictly positive. Thus, the implied volatility smiles in terms of the standardized moneyness z are flat at both very short and very long maturities. The short-maturity behavior is driven by the continuous price assumption, whereas the long-maturity behavior is governed by the central limit theorem under the return volatility stationarity assumption.

At an intermediate time to maturity τ, the implied volatility smile $v_t(\tau,z)$ is a hyperbola, which is asymptotically linear in z, with the asymptotic slopes given by

$$\lim_{z\to\pm\infty} \frac{\partial v_t(z,\tau)}{\partial z} = \frac{w_t e^{-\eta_t\tau}\sqrt{\tau}\left(-w_t e^{-\eta_t\tau}\tau \pm \sqrt{w_t^2 e^{-2\eta_t\tau}\tau + 4\left(1+\kappa_t\tau\right)}\right)}{2\left(1+\kappa_t\tau\right)}. \tag{25}$$

On the other hand, around the at-the-money point ($z = 0$), the slope of the smile is mainly determined by the instantaneous correlation ρ_t between the stock return and implied volatility,

$$\left.\frac{\partial v_t(z,\tau)}{\partial z}\right|_{z=0} = \frac{\left(\rho_t - \frac{1}{2}w_t e^{-\eta_t\tau}\tau\sqrt{\zeta_t}\right) w_t e^{-\eta_t\tau}\sqrt{\tau}}{\left(1+\kappa_t\tau\right)\sqrt{\zeta_t}}, \tag{26}$$

with $\zeta_t = \left(1 + \frac{\left(\theta_t - w_t^2 e^{-2\eta_t\tau}/\kappa_t\right)}{s_t^2}\kappa_t\tau\right) / \left(1+\kappa_t\tau\right)$.

For at-the-money implied volatilities with $z = 0$, equation (22) reduces to

$$\left(1+\kappa_t\tau\right) a_t^2(\tau) - \left[\left(\kappa_t\theta_t - w_t^2 e^{-2\eta_t\tau}\right)\tau + s_t^2\right] = 0. \tag{27}$$

Thus, the at-the-money implied variance term structure is given by

$$a_t^2(\tau) = \frac{\left(\kappa_t\theta_t - w_t^2 e^{-2\eta_t\tau}\right)\tau + s_t^2}{\left(1+\kappa_t\tau\right)}. \tag{28}$$

Interestingly, although equation (20) shows that the at-the-money implied volatility term structure does not depend on the volvol process ω_t, the at-the-money implied volatility term structure defined

in (28) does depend on the volatility of the implied variance dynamics w_t because the volatility of the implied variance enters into the drift of the implied volatility dynamics. If we reparameterize the drift of the implied volatility dynamics as

$$\mu_t = \frac{1}{2}\left(\frac{\alpha_t}{I_t(K,T)} - \beta_t I_t(K,T)\right), \tag{29}$$

with $\alpha_t = \kappa_t\theta_t - w_t^2 e^{-2\eta_t\tau}$ and $\beta_t = \kappa_t$, the at-the-money implied variance term structure can be written as,

$$a_t^2(\tau) = \frac{\alpha_t\tau + s_t^2}{1+\beta_t\tau}, \tag{30}$$

free of dependence on the volvol coefficients.

1.4. Implied volatility as a function of log moneyness and term

In the OTC equity index derivatives market, the moneyness is often represented in terms of the log strike over spot, $k_t \equiv \ln(K/S_t)$, instead of the standardized moneyness measure in (5). Let $\hat{I}_t(k,\tau) \equiv v_t(z,\tau)$ denote the implied volatility surface as a function of this log moneyness and time to maturity. The following proposition describes the algebraic restriction on the implied volatility surface function $\hat{I}_t(k,\tau)$.

Proposition 4 *When the implied volatility surface is represented in terms of the log moneyness k and the time to maturity* τ*, the algebraic relation on the implied volatility function becomes,*

$$\frac{s_t^2}{2} - \frac{\hat{I}_t^2(k,\tau)}{2} + [\mu_t\hat{I}_t(k,\tau) + \frac{\rho_t\omega_t s_t}{2}\hat{I}_t(k,\tau)]\tau + \frac{\rho_t\omega_t s_t}{\hat{I}_t(k,\tau)}k - \frac{\omega_t^2}{8}\hat{I}_t^2(k,\tau)\tau^2 + \frac{\omega_t^2}{2\hat{I}_t^2(k,\tau)}k^2 = 0. \tag{31}$$

Proof. The proof follows readily if we start with equation (18) and replace z with the following representation in terms of k and $\hat{I}_t(k,\tau)$,

$$z = \frac{k}{\hat{I}_t(k,\tau)\sqrt{\tau}} + \frac{\hat{I}_t(k,\tau)\sqrt{\tau}}{2}. \tag{32}$$

■

Corresponding to this new representation of the implied volatility surface, we propose an alternative implied variance dynamics,

$$dI_t^2(K,T) = \kappa_t[\theta_t - I_t^2(K,T)]dt + 2w_t e^{-\eta_t(T-t)} I_t^2(K,T)dZ_t, \tag{33}$$

which is mean-reverting with log-normal volatility, with κ, θ, w, and η being nonnegative stochastic processes that do not depend on K, T, or $I(K,T)$. As in (21), we furthermore assume that η is strictly positive to maintain stationarity.

Proposition 5 *Under the stock price dynamics in (1)-(3), when the implied variance follows the mean-reverting lognormal dynamics in (33), the implied variance surface satisfies the following quadratic equation,*

$$\begin{aligned} &\tfrac{w_t^2}{4} e^{-2\eta_t\tau}\tau^2 \hat{I}_t^4(k,\tau) + \left[1 + \kappa_t\tau + w_t^2 e^{-2\eta_t\tau}\tau - \rho_t s_t w_t e^{-\eta_t\tau}\tau\right] \hat{I}_t^2(k,\tau) \\ &- \left[s_t^2 + \kappa_t\theta_t\tau + 2\rho_t s_t w_t e^{-\eta_t\tau}k + w_t^2 e^{-2\eta_t\tau}k^2\right] = 0. \end{aligned} \tag{34}$$

Proof. Applying Ito's lemma on (33), we obtain the dynamics for the implied volatility as,

$$dI_t(K,T) = \frac{1}{2}\left[\frac{\kappa_t\theta_t}{I_t(K,T)} - \left(\kappa_t + w_t^2 e^{-2\eta_t(T-t)}\right) I_t(K,T)\right] dt + w_t e^{-\eta_t(T-t)} I_t(K,T)dZ_t. \tag{35}$$

Hence, the risk-neutral drift and the volvol processes are

$$\mu_t = \frac{1}{2}\left(\frac{\kappa_t\theta_t}{\hat{I}_t(k,\tau)} - \left(\kappa_t + w_t^2 e^{-2\eta_t(T-t)}\right)\hat{I}_t(k,\tau)\right), \quad \omega_t = w_t e^{-\eta_t(T-t)}\hat{I}_t(k,\tau), \tag{36}$$

where $\hat{I}_t(k,\tau) \equiv I_t(K,T)$. Substituting (36) into the no dynamic arbitrage restriction (31) leads to the quadratic equation for implied variance in (34). ■

Given the coefficients $(\kappa_t, w_t, \eta_t, \theta_t, s_t, \rho_t)$, we can solve the whole implied variance surface analytically as a solution to the quadratic equation in (34). We take the positive root as the solution for the implied variance, and we label this class of implied variance surfaces as the **lognormal variance (LNV)** model.

The equation in (34) describes a hyperbola in the variables $\hat{I}^2$ and k, a property that also arises in the Gatheral (2006) SVI parametrization. The relation dictates that the implied variance $\hat{I}_t^2$ is convex in k. Furthermore, as $k \to \pm\infty$, the implied variance smile behaves linearly in log moneyness k. This asymptotic linearity of implied variance $\hat{I}_t^2$ in log moneyness is consistent with the no arbitrage condition derived by Lee (2004). In particular, if we use

$$\gamma_\pm = \lim_{k\to\pm\infty} \sup \frac{\hat{I}_t^2(k,\tau)\tau}{|k|}, \tag{37}$$

to denote the asymptotic slopes of the implied variance, Lee shows that the asymptotic slopes must be within $[0,2]$ to exclude arbitrage and that they define the maximum finite moments of the stock price in the following sense,

$$\begin{aligned} p_+ &\equiv \sup\{p_+ : \mathbb{E}[S_T^{1+p_+}] < \infty\} = \tfrac{1}{2}\left(\tfrac{1}{\sqrt{\gamma_+}} - \tfrac{\sqrt{\gamma_+}}{2}\right)^2, \\ p_- &\equiv \sup\{p_- : \mathbb{E}[S_T^{-p_-}] < \infty\} = \tfrac{1}{2}\left(\tfrac{1}{\sqrt{\gamma_-}} - \tfrac{\sqrt{\gamma_-}}{2}\right)^2. \end{aligned} \tag{38}$$

The LNV model has the same asymptote at both sides $\gamma_\pm = 2$, which is at the boundary of the no-arbitrage limit, with $p_\pm = 0$.

In the limit of $\tau = 0$, the implied variance is quadratic in the log strike moneyness k,

$$\hat{I}_t^2(k,0) = s_t^2 + 2\rho_t s_t w_t k + w_t^2 k^2, \tag{39}$$

where the curvature is determined by the volvol coefficient w and the asymmetry is determined by the correlation ρ. It is interesting to note that although implied volatility as a function of the standardized moneyness z is flat at zero maturity under continuous price dynamics, it does not need to be flat in k.

When $z = 0$ and hence $k = -\frac{1}{2}\hat{I}_t^2(k,\tau)\tau$, we obtain the at-the-money implied variance term structure $a_t(\tau) = \hat{I}_t^2(-\frac{1}{2}\hat{I}_t^2(k,\tau)\tau,\tau)$ as,

$$a_t(\tau)^2 = \frac{\kappa_t\theta_t\tau + s_t^2}{1 + \left(\kappa_t + w_t^2 e^{-2\eta_t\tau}\right)\tau}. \tag{40}$$

When we reparameterize the drift of the implied volatility process as $\mu_t = \frac{1}{2}\left(\frac{\alpha_t}{\hat{I}(k,\tau)} - \beta_t \hat{I}_t(k,\tau)\right)$, with $\alpha_t = \kappa_t\theta_t$ and $\beta_t = \kappa_t + w_t^2 e^{-2\eta_t\tau}$, the at-the-money implied variance term structure can be represented as,

$$a_t^2(\tau) = \frac{\alpha_t\tau + s_t^2}{1 + \beta_t\tau}, \tag{41}$$

again free of dependence on the volvol coefficients. The at-the-money implied variance starts at the instantaneous variance s_t^2 at $\tau = 0$ and converges to θ as the maturity approaches infinity.

2. Dynamic Calibration of Implied Volatility Surfaces

For both the SRV and the LNV specifications under the VGVV framework, we use six coefficients $X_t \equiv (\kappa_t, w_t, \eta_t, \theta_t, s_t, \rho_t)^\top$ to describe a whole implied volatility surface across all strikes and maturities. We can calibrate the values of these six coefficients from a finite number of implied volatility

quotes, with which we can build up the whole implied volatility surface and determine its future risk-neutral dynamics. In this section, we propose a dynamic approach in calibrating the implied volatility surfaces over different days t. In this approach, we regard the six ($k = 6$) coefficients X_t as the hidden state, and the finite number (n) of implied volatility quotes as our observations. We build a state-space structure, and infer the hidden states from the observations each day using a filtering approach.

Specifically, we assume that the states propagate according to a random walk process,

$$X_t = X_{t-1} + \sqrt{\Sigma_x}\varepsilon_t, \tag{42}$$

where we assume that the standardized error ε_t is normalized distributed with zero mean and unit variance. We further assume that the covariance matrix is a diagonal matrix so that the coefficients can have different degrees of variations but the movements are independent of each other.

In reality, the six coefficients represent six different processes, which can follow much more complex dynamics than assumed in the state propagation equation in (42). The purpose of the simplified state propagation equation is to set up a framework where we retain the last states and hence the last calibrated implied volatility surface until we have new observations. Furthermore, the six coefficients have different allowable value ranges, as $(\kappa_t, w_t, \eta_t, \theta_t, s_t)$ must be positive and ρ_t between $[-1, 1]$. We transform these coefficients such that they can all take values on the whole real line. Specifically, we take natural logs on $(\kappa_t, w_t, \eta_t, \theta_t, s_t)$ and we translate the correlation coefficient by $x_\rho = \ln(1+\rho)/(1-\rho)$. In estimation, the states are defined on these transformed coefficients.

We define the measurement equations on the observed implied volatility quotes, assuming

additive, normally distributed errors,

$$y_t = h(X_t) + \sqrt{\Sigma_y} e_t, \tag{43}$$

where $y_t \in \mathbb{R}^{n+}$ denotes the n implied volatility quotes on date t and $h(X_t)$ denotes its model value as a function of the coefficients X_t. The function is given by the positive solution to the quadratic equation in (22) under the SRV model and the positive solution to the quadratic equation in (34) under the LNV model. In estimation, we give more weight to at-the-money implied volatilities than out-of-the-money implied volatilities by applying an exponentially decaying weight based on the log relative strike $e^{-k^2/2}$. Then, we assume that the weighted pricing errors are iid normally distributed with error variance σ_e^2. Thus, $\Sigma_y = I_n \sigma_e^2$, with I_n denoting an identity matrix of dimension n. This setup introduces seven auxiliary parameters Θ that define the covariance matrix of the state and the measurement errors.

When the state propagation and the measurement equation are Gaussian linear, the Kalman (1960) filter provides efficient forecasts and updates on the mean and covariance of the state and observations. Our state-propagation equations are Gaussian and linear, but the measurement functions $h(X_t)$ are not linear in the state vector. We use the unscented Kalman filter to handle the nonlinearity. Specifically, we start with the linear Gaussian prediction on the state vector,

$$\overline{X}_t = \widehat{X}_{t-1}, \quad \overline{V}_{x,t} = \widehat{V}_{x,t-1} + \Sigma_x, \tag{44}$$

where $\overline{X}_t$ and $\overline{V}_{x,t}$ are the time-$(t-1)$ predicted value of the conditional mean and covariance matrix of the state vector. Based on these predictions, we draw a set of $2k+1$ sigma vectors χ_i on the state, with k denoting the dimension of the state space,

$$\chi_{t,0} \;=\; \overline{X}_t, \quad \chi_{t,i} = \overline{X}_t \pm \sqrt{(k+\delta)(\overline{V}_{x,t})_j} \tag{45}$$

where the weights are given by $w_0 = \delta/(k+\delta)$ and $w_i = 1/[2(n+\delta)]$ for $i > 0$, with δ being a control parameter. We propagate the sigma points through the nonlinear measurement equation to obtain a set of sigma points on the measurements, $\zeta_{t,i} = h(\chi_{t,i})$, with which we compute the predicted mean $\overline{y}_t$ and covariance matrix $\overline{V}_{y,t}$ of the measurement series, as well as the covariance matrix between the state vector and the measurement $\overline{V}_{xy,t}$:

$$\begin{aligned} \overline{y}_t &= \textstyle\sum_{i=0}^{2k} w_i \zeta_{t,i}, \\ \overline{V}_{y,t} &= \textstyle\sum_{i=0}^{2k} w_i \left[\zeta_{t,i} - \overline{y}_t\right] \left[\zeta_{t,i} - \overline{y}_t\right]^\top + \Sigma_y, \\ \overline{V}_{xy,t} &= \textstyle\sum_{i=0}^{2k} w_i \left[\chi_{t,i} - \overline{X}_t\right] \left[\zeta_{t,i} - \overline{y}_t\right]^\top. \end{aligned} \tag{46}$$

Using these moment conditions, we apply the Kalman filter to obtain the filtered values of the mean $\widehat{X}_t$ and covariance $\widehat{V}_{y,t}$ of the state vector:

$$\widehat{X}_t = \overline{X}_t + K_t\left(y_t - \overline{y}_t\right), \quad \widehat{V}_{x,t} = \overline{V}_{yx,t} - K_t \overline{V}_{y,t} K_t^\top, \tag{47}$$

where $K_t = \overline{V}_{xy,t}\left(\overline{V}_{y,t}\right)^{-1}$ denotes the Kalman gain. We refer the reader to Wan and van der Merwe (2001) for general treatments of the unscented Kalman filter.

Given the filtered values of the states $\widehat{X}_t$, we compute the fitted values of the implied volatility observations, $\widehat{y}_t = h(\widehat{X}_t)$, and define the sum squared fitting error (SSE) at each date t as,

$$l_t = \left(y_t - \widehat{y}_t\right)^\top \left(y_t - \widehat{y}_t\right). \tag{48}$$

We choose the values of the auxiliary parameters Θ to minimize the summation of the daily SSE's over the whole sample period,

$$\Theta \equiv \arg\min_{\Theta} \mathcal{L}(\Theta, \{y_t\}_{t=1}^N), \quad \text{with} \quad \mathcal{L}(\Theta, \{y_t\}_{t=1}^N) = \sum_{t=1}^{N} l_t(\Theta), \tag{49}$$

where N denotes the number of days in our sample. Once the auxiliary parameters are estimated on a training sample, the unscented Kalman filter can be used to provide fast sequential calibration of the implied volatility surface over different days.

The closest counterpart in the traditional option pricing literature to our two models (SRV and LNV) is the stochastic volatility model of Heston (1993), which specifies a pure diffusion dynamics for the stock price and a mean-reverting square-root process for the instantaneous variance rate:

$$dS_t/S_t = s_t dW_t, \quad ds_t^2 = \kappa(\theta - s_t^2)dt + w s_t dZ_t, \quad \rho dt = \mathbb{E}[dW_t dZ_t]. \tag{50}$$

Under this model, the implied volatility surface on a given date is determined by five coefficients, including four fixed parameters $(\kappa, \theta, w, \rho)$ and the instantaneous variance rate s_t^2. For comparison, we also calibrate the Heston model to match the daily observations of implied volatility surfaces. To make the models comparable, we allow the fixed parameters in the Heston model to vary over time so that the model has five coefficients each day to match the observed implied volatility surface. For model estimation, we regard the five coefficients as the hidden states and perform similar transformations on the coefficients so that they take values on the whole real line. In this case, the value function $h(X_t)$ in the measurement equation (43) is no longer analytical; instead, it involves a numerical integration of the Fourier transform of the stock return to obtain the options value. A numerical root-finding routine is further needed to convert the option value into an implied volatility. To mitigate the computational burden, we perform preprocessing on the data and convert the implied volatility quotes into out-of-the-money option values in percentages of the spot, we further scale each option value by the BMS vega of the option, and regard the scaled option value as the measurement series y_t with identical error variance. Even after this preprocessing, calibrating the Heston model can be about 100 times slower than calibrating the two implied volatility models SRV and LNV. The Heston model is widely regarded as the most analytically tractable stochastic volatility specification in the option pricing literature. Its computational complexity and speed dif-

ference from our two models highlight the extreme simplicity and tractability of our specification.

3. Application to Currency Option Implied Volatility Surfaces

Over-the-counter quotes on currency options are typically in terms of BMS implied volatilities for delta-neutral straddles and 10- and 25-delta risk reversals and butterfly spreads at fixed time to maturities. A straddle is a portfolio of a call option and a put option with the same strike. The strike of the delta-neutral straddle is chosen to make the BMS delta of the straddle zero:

$$\Delta_c + \Delta_p = 0, \tag{51}$$

where Δ_c and Δ_p denote the BMS delta of the call option and the put option in the straddle, respectively,

$$\Delta_c = e^{-r_f \tau} N[-z^S + v^S \sqrt{\tau}], \quad \Delta_p = -e^{-r_f \tau} N[z^S - v^S \sqrt{\tau}], \tag{52}$$

with $N[\cdot]$ denoting the cumulative normal function, v^S denoting the straddle implied volatility, r_f denotes the continuously compounding spot interest rate for the foreign currency at the corresponding maturity, and z^S denotes the standardized moneyness measure for the straddle. Combining the delta-neutrality condition in (51) with the BMS delta definitions in (52) solves the standardized moneyness measure for the straddle as,

$$z^S = v^S \sqrt{\tau}. \tag{53}$$

A 10-delta risk reversal is a portfolio composed of a long position in the 10-delta call option and a short position in the 10-delta put at the same maturity. The 10-delta risk reversal quote, RR^{10},

reflects the the BMS implied volatility difference between the 10-delta call and the ten-delta put,

$$RR^{10} = v^{10c} - v^{10p}. \tag{54}$$

Risk reversals at other deltas are analogously defined.

A 10-delta butterfly spread is a portfolio composed of long position in the 10-delta call and the 10-delta put option and short position in the delta-neutral straddle. The butterfly quote measures the BMS implied volatility difference between the two out-of-the-money options and the straddle,

$$BF^{10} = \left(v^{10c} + v^{10p}\right)/2 - v^{S}. \tag{55}$$

Risk reversal and butterfly quotes at other deltas are analogously defined.

From the straddle, risk reversal, and butterfly spread quotes, we can infer the implied volatilities at the four moneyness levels,

$$\begin{array}{rclcrcl} v^{10c} &=& BF^{10} + v^{S} + \frac{1}{2}RR^{10}, & & v^{10p} &=& BF^{10} + v^{S} - \frac{1}{2}RR^{10}, \\ v^{25c} &=& BF^{25} + v^{S} + \frac{1}{2}RR^{25}, & & v^{25p} &=& BF^{25} + v^{S} - \frac{1}{2}RR^{25}, \end{array} \tag{56}$$

and the corresponding values for the standardized moneyness measures (z) are

$$\begin{array}{rclcrcl} z^{10c} &=& -N^{-1}\left(0.1e^{r_f\tau}\right) + v^{10c}\sqrt{\tau}, & & z^{10p} &=& N^{-1}\left(0.1e^{r_f\tau}\right) + v^{10p}\sqrt{\tau}, \\ z^{25c} &=& -N^{-1}\left(0.25e^{r_f\tau}\right) + v^{25c}\sqrt{\tau}, & & z^{25p} &=& N^{-1}\left(0.25e^{r_f\tau}\right) + v^{25p}\sqrt{\tau}, \end{array} \tag{57}$$

where $N^{-1}(\cdot)$ denotes the inverse of the cumulative normal function. Therefore, from the OTC currency option quotes, we can readily obtain observations on the implied volatility surface as a function of the standardized moneyness z and time to maturity τ. We can also convert the standardized moneyess measure z into log strike over forward, k.

The definitions of risk reversals and butterfly spreads in (54) and (55) are based on a simplified industry convention, with which the implied volatilities at the corresponding deltas can be solved uniquely as shown in (56). The industry sometimes applies more complex conventions, where the butterfly and risk reversal at the same delta may refer to different strikes and as a result computing implied volatilities from risk reversal and butterfly spread quotes depend on interpolation assumptions. The data we obtain are already converted into implied volatilities. In this case, we use the simplified risk reversal and butterfly spreads definitions in (54) and (55) as an intuitive way to represent the skew and curvature of the implied volatility smile at a fixed time to maturity.

3.1. Data description and summary statistics

We obtain BMS implied volatility quotes on two currency pairs, dollar price of yen (USDJPY) and dollar price of pound (GBPUSD), from an investment bank. The data are from January 8, 1997 to December 26, 2007, sampled weekly on every Wednesday. At each date, quotes are available at five deltas (delta-neutral straddle, 10- and 25-delta calls and puts) and across 11 maturities at one, two, three, six, nine, 12, 18, 24, 36, 48, and 60 months. All together,573 weekly observations are available on 55 series for a total of 31,515 observations.

To calibrate the SRV model and the LNV model, we directly use the implied volatilities quotes, as a function of the standardized moneyness z and time to maturity τ for the SRV model and as a function of log strike over forward k and time to maturity τ for the LNV model. To calibrate the Heston model for comparison, we convert the implied volatility quotes into forward out-of-the-money option values in percentages of the forward and scaled by the BMS vega. These option values are represented as a function of relative strikes in percentages of forward (K/F) and time to maturity. The relative strikes can be directly computed from the standardized moneyness measure and the corresponding implied volatility quote. In these calculations, maturity-matched continuously compounded spot interest rates on dollar, yen, and pound are constructed using LIBOR

(London Interbank Offer Rates) and swap rates taken from Bloomberg.

Table 1 reports the summary statistics of the implied volatility quotes. Panel A reports the sample averages of the implied volatilities. For dollar-yen, the 10- and 25-delta call implied volatilities are on average higher than the put counterparts across all maturities. Thus, the risk reversals are on average positive for this currency pair, indicating that the conditional risk-neutral return distribution of the dollar price of yen is positively skewed on average. By contrast, the sample averages of the call and put implied volatilities for dollar-pound currency pair are much more symmetric. For both currency pairs, the out-of-the-money implied volatilities are on average higher than the delta-neutral straddle implied volatilities. Butterfly spreads are positive on average.

[Table 1 about here.]

Figure 1 plots the average implied volatility smile as a function of put delta, with 10- and 25-delta call implied volatilities approximated as implied volatilities for 90- and 75-delta puts. Each panel is for one currency pair and the four lines in each panel denote four selected maturities at one month (solid lines), three months (dashed lines), one year (dash-dotted lines), and five years (dotted lines). The average implied volatility shapes are very similar to one another for maturities within one year, whereas the shapes of the five-year average implied volatility smile show some variation. The average smiles for dollar-yen are positively skewed, and the average skew becomes more positive for five-year options. The average smiles for dollar-pound are more symmetric, with the five-year smiles averaging higher but flatter than smiles at shorter maturities.

[Figure 1 about here.]

Table 1 reports the standard deviation estimates of the implied volatility quotes in panel B. The estimates decline steadily with increasing time to maturities for both currency pairs, justifying strictly positive volatility discounting coefficients η for both SRV and LNV models. Panel C

reports the weekly autocorrelation of the implied volatility quotes. All implied volatility series are persistent, more so for long-dated series than short-dated series.

Figure 2 plots the time series of the delta-neutral straddle implied volatilities at different maturities, which show strong co-movements across maturities. The straddle implied volatilities on dollar-yen experienced a large spike during the 1998 hedge fund crisis and have been trending down since then, until the pickup in late 2008 as the new financial crisis started to propagate. The implied volatilities on dollar-pound varied within a much narrower range between 5-13%.

[Figure 2 about here.]

Figure 3 plots the time series of the 10-delta risk reversals and butterfly spreads. Both risk reversals and butterfly spreads vary strongly over time. Intuitively, risk reversal provide a simple slope measure of the implied volatility smile across delta, whereas the butterfly spread provide a measure of the curvature of the smile. The strong time variations suggest that the conditional risk-neutral return skewness and kurtosis vary strongly over time. Carr and Wu (2007) provide a systematic documentation on the strong variation in the risk reversals and develop a class of stochastic skew models that can capture this variation. Bakshi, Carr, and Wu (2008) explore the implication of the stochastic skew on the variation of risk premiums in different economies. Our data over a more extended period show that both the risk reversal and the butterfly spreads vary strongly over time. While the risk reversals often switch signs, the butterfly spreads always stay positive, suggesting that while the risk-neutral return distribution can switch from positive to negatively skewed, the distribution always show positive excess kurtosis.

[Figure 3 about here.]

Before May 31, 2000, the 10-delta risk reversals and butterfly spreads at five-year maturity (in dash-dotted lines) were set to zero. Thus, long-term implied volatilities were quoted as flat

across moneyness. This flat quotation convention has been abandoned since then. For dollar-yen, the five-year 10-delta risk reversals have stayed positive since then and have become more positive than risk reversals at shorter maturities. The five-year 10-delta butterfly spreads have also become more positive than butterfly spreads at shorter maturities since 2004. For dollar-poind, as the risk reversals at short maturities switch signs, the long-term risk reversals reversals follow the same trend, but with less variation. The butterfly spreads on dollar-pound are not updated as frequently until very recently. The spreads at five years become more positive than spreads at shorter maturities since 2005. The recent increase in risk reversals and butterfly spreads at long maturities reflects growing apprehension in the currency options market of the risks on long-dated out-of-the-money options.

3.2. Pricing performance comparisons

Tables 2 reports the summary statistics of the pricing errors on dollar-yen option implied volatilities from the three models. The pricing errors are defined as the difference between the implied volatility quotes and the corresponding model values, both in percentage volatility points. Panel A reports the root mean squared pricing errors for each series, which average at 0.40 volatility point for the SRV model, and 0.36 volatility point for the LNV model, and 0.37 volatility point for the Heston model. At a fixed maturity, the errors are larger for out-of-the-money options than for at-the-money options. At a fixed delta, errors are larger at very short or long maturities than at intermediate maturities, For all three models, the largest errors come from one-month 10-delta call options.

[Table 2 about here.]

Panel B reports the explained variation, defined as one minus the ratio of pricing error variance to the variance of the implied volatility series. The explained variation estimates average at 98% for

the SRV model and the Heston model, and slightly higher at 99% for the LNV model. These high explained variation and low root mean square estimates suggest that all three models with time-varying coefficients can capture the majority variation of the dollar-yen option implied volatility surface, with the LNV model performing slightly better than the other two models.

Panel C reports the weekly autocorrelation on the pricing errors, which averages at 0.80 for the SRV model, 0.78 for the LNV model, and 0.85 for the Heston model. For investors who wish to generate trading opportunities based on the deviation between market observations and model valuations, a key criterion for a good model is to generate pricing errors with low serial persistence so that the deviations can converge quickly over time. Based on this criterion, the LNV model also performs slightly better than the other two models.

Tables 3 reports the summary statistics of the pricing errors on dollar-pound option implied volatilities from the three models. The pricing errors are smaller on dollar-pound options than on dollar-yen options. The root mean squared pricing errors average at 0.13 volatility point for the SRV model, 0.12 volatility point for the LNV model, and 0.14 volatility point for the Heston model. The explained variation estimates average at 99% for the SRV model and the LNV model, and 98% for the Heston model. The weekly autocorrelation estimates on the pricing errors average at 0.73 for the SRV model, 0.74 for the LNV model, and 0.78 for the Heston model. Overall, all three models perform well in capturing the dollar-pound implied volatility surface behavior. Among the three models, the LNV model generates the best performance in terms of smaller root mean squared pricing errors, larger explained variation, and low serial correlation for the pricing errors.

[Table 3 about here.]

3.3. Time-varying implied volatility dynamics

Figure 4 plots the time series of the model coefficients calibrated to the dollar-yen option implied volatilities. For each model, we group the coefficients into three panels from top to bottom. The three columns are for the three different models. The top panels plot the time series of the short- and long-run volatility level, s_t (solid lines) and $\sqrt{\theta_t}$ (dashed lines), both represented in volatility percentage points. As expected, the instantaneous volatility s_t shows more transient movements than the long-run trend θ. The spike in s_t in late 1998 corresponds to the spike in the straddle implied volatilities during the hedge fund crisis. Among the three models, he estimates on the LNV model show the most stability. The Heston model generates larger short-term volatility estimates during the spikes, whereas the SRV model estimates for s_t and $\sqrt{\theta_t}$ show some separation between 2005 and 2007.

[Figure 4 about here.]

The middle panels plot the time series of the mean-reversion coefficient κ_t, the volvol coefficient w_t, and for SRV and LNV models, the volvol decay coefficient η_t. The mean-reversion speed κ_t is much larger in scale than the volvol coefficient and the volvol decay coefficient. Thus, we scale κ by 20 so that we can plot them in the same panel. Under both SRV and LNV models, the estimates for the volvol decay coefficient η_t are much larger before 2000 and than after. The shift in the η_t estimates captures the shift in the long-dated implied volatility smile quotes. A larger η_t contributes to a faster convergence to a flat implied volatility smile. After 2000, the long-dated butterfly spreads and risk reversals tend to be as large as the short-dated values, as a result, the η_t estimates become close to zero as a way to slow down the convergence speed of the central limit theorem. With η_t capturing this structural shift in the implied volatility smiles, the estimates for both κ_t and w_t become reasonably stable over time for the SRV and the LNV models. By contrast, since the Heston model does not have this separate decay coefficient, the estimates for κ_t and w_t

vary more over time.

The bottom three panels of Figure 4 plot the time series of the correlation coefficients between the diffusions in return and volatility. The estimates show large variation to capture the time variation of the risk reversals. The coefficients frequently switch signs during the first half but become increasing positive during the second half, reflecting the increasing asymmetry between the two economies.

Figure 5 plots the time series of the model coefficients calibrated to the dollar-pound option implied volatilities. As for dollar-yen options, the top panels show that the short-term volatility (s_t) varies around the long-term trend $\sqrt{\theta_t}$ for dollar-pound options. The middle panels show that both the mean-reversion speed and the volvol coefficients reached a peak in 2000, corresponding to a period of strong variation in dollar-pound straddle implied volatilities. Finally, the bottom panels show that the correlation coefficients vary around zero and frequently switch signs, consistent with the behavior of dollar-pound risk reversals.

[Figure 5 about here.]

4. Application to S&P 500 Index Option Implied Volatilities

Different from the OTC currency options market, the OTC equity index options market often provide quotes with fixed time to maturity and fixed relative strike in percentage of the spot. We obtain OTC implied volatility quotes on the S&P 500 index (SPX) options from an investment bank. The sample for the equity index options covers the same time period as for the currency options, from January 8, 1997 to December 26, 2007 for 573 weeks. At each date, the equity index option implied volatility quotes are available at eight fixed time to maturities at one, three, six, 12, 24, 36, 48, and 60 months. At each maturity, the implied volatilities are quoted at five relative strikes at

80, 90, 100, 110, and 120 percent of the spot index level. All together, the sample contains 40 implied volatility series on a grid of five relative strikes and eight fixed time to maturities over 573 weeks, a total of 22,920 data points.

4.1. Statistical behavior of SPX option implied volatilities

Table 4 reports the summary statistics of the implied volatility quotes. Panel A reports the sample averages of the implied volatilities. At each fixed maturity, the average implied volatilities decline with increasing strike prices, generating the well-documented implied volatility skew pattern for the stock index. At each fixed relative strike (K/S), the implied volatilities increase with the time to maturity for at-the-money options (100% strike) and at high relative strikes (110% and 120% strikes), but the term structure becomes downward sloping for options at 80% and 90% relative strikes.

[Table 4 about here.]

Panel B of Table 4 reports the standard deviation estimates of the implied volatility series. Consistent with the negative skew in the implied volatility levels, the standard deviation estimates also decline with increasing strikes. Along the maturity dimension, the standard deviation estimates show a steeply downward sloping term structure, consistent with our exponential decay specification on volvol process. Panel C of Table 4 reports the weekly autocorrelation estimates of the implied volatility series. The estimates range from 0.936 to 0.989. Overall, the long-dated implied volatilities are more persistent than short-dated implied volatilities.

Figure 6 plots the time series of the at-the-money spot implied volatility in the left panel, where the three lines represent three selected maturities at one month (solid line), one year (dashed line), and five years (dash-dotted line). Short-term implied volatilities show more time variation than long-term implied volatilities. During our sample period, the one-month at-the-money implied

volatility has varied from as low as 8.67% on January 24, 2007 to as high as 41.63% on October 7, 2998. By contrast, the five-year at-the-money implied volatility has varied within a narrower range from 14.90% on January 1, 2004 to 35.82% on October 14, 1998. The long-term volatility tends to stay above the short-term volatility except during crisis times when the short-term volatility shoots over the long-term level.

[Figure 6 about here.]

To compare the implied volatility skew at different maturities, we compute a standardized implied volatility skew measure, defined as the implied volatility difference between 80% and 120% strike, normalized by the corresponding difference in the standardized moneyness measure z. The right panel of Figure 6 plots the time series of this skew measure at three selected maturities at one month (solid line), one year (dashed line), and five years (dash-dotted line). Across the whole sample period and across all maturities, the implied volatilities are negatively skewed across moneyness, suggesting that the conditional risk-neutral SPX return distribution is negatively skewed at all times and all conditioning horizons. Furthermore, the conditional return distribution is more negatively skewed at long maturities than at short maturities on most days. Only on a few exceptions does the skew term structure switch directions.

4.2. Pricing performance comparison on SPX option implied volatilities

Table 5 reports the summary statistics of the pricing errors on the equity index option implied volatilities from the three models. The root mean squared pricing errors average at 0.87 volatility point for the SRV model, 0.67 volatility point for the LNV model, and 1.12 volatility point for the Heston model. For all three models, the pricing errors in implied volatilities are larger at short maturities. Panel B reports the explained variation, which averages at 99% for the SRV model and the LNV model, and 95% for the Heston model. Panel C reports the weekly autocorrelation of the

pricing errors, which averages at 0.84 for the SRV model, 0.77 for the LNV model, and 0.85 for the Heston model.

[Table 5 about here.]

Taken together, our extensive calibration exercise on 11 years of implied volatility surfaces for two currency pairs and one equity index shows that with five to six time-varying coefficients, both the two implied volatility models (SRV and LNV) and the Heston model perform reasonably well in capturing the major variations in the implied volatility surface across all three underlying securities. Among the three models, the LNV model performs the best in generating smaller root mean squared pricing errors, larger explained variation, and lower serial dependence in its pricing errors. More importantly, the SRV model and the LNV model are much simpler to implement because generating implied volatility surfaces from these two models does not involve numerical integration or nonlinear minimization. As a result, constructing implied volatility surfaces using the SRV and LNV model is 100 times faster than using the Heston model.

4.3. Time-varying implied volatility dynamics

Figure 7 plots the time series of the model coefficients calibrated to the SPX options. The top panels show that for SPX options, the long-run trend θ tend to stay above the instantaneous volatility level s_t to capture the mostly upward sloping at-the-money implied volatility term structure, observed in the left panel of Figure 6. This is particularly the case under the LNV model.

[Figure 7 about here.]

The middle panels show another distinct feature of the equity index options: The dynamics show much smaller mean reversion and even smaller volvol coefficients. For the two implied

volatility models, the volvol decay coefficients are virtually zero. The small estimates are needed to capture the increasingly negative skew at long maturities as shown in the right panel of Figure 6. Large estimates for the mean reversion speed κ and volvol decay coefficient η generate faster convergence to return normality as the option maturity increases. To accommodate the fact that the risk-neutral return distribution is even more negatively skewed at five years than at one month, one needs near non-stationarity in the implied volatility dynamics to slow down the effect of central limit theorem.

The bottom panels show that the correlation coefficients are always negative and almost always lower than -0.5, in line with the persistently negative skewness observed in the equity index options. The time-series variation of the correlation estimates are in general alliance with the time-series variation of the skewness measure we have plotted in the right panel of Figure 6.

5. Concluding Remarks

Despite the fact that the BMS model assumptions are obviously violated, practitioners are deeply entrenched in BMS implied volatilities. They do so for several good reasons because the implied volatilities are more stable and more revealing about the underlying return dynamics than the option prices do. Quoting a positive implied volatility for an option contract also directly excludes arbitrage between this option and the underlying security, adding further attraction to the implied volatility quoting convention.

Given this quoting convention, it would be ideal if one can directly model the implied volatility dynamics and derive direct implications on the shape of the implied volatility surface. Market models of implied volatilities attempt to model the martingale component of the implied volatility dynamics while taking the initial implied volatility surface as given. However, the shape of the implied volatility surface can put severe constraints on what the implied volatility dynamics can be.

In this paper, we directly model both the drift and the martingale component of the implied volatility dynamics, and we derive the dynamic-no-arbitrage implication of our assumed dynamics on the shape of the implied volatility surface. By design, our approach guarantees the dynamic consistency between the implied volatility dynamics and the derived implied volatility surface shape. To the extent that market observations can differ from the model-implied surface, the deviations can serve as relative trading opportunities.

Our new approach generates very promising results. We consider two parametric specifications for the implied volatility dynamics, and both lead to extremely simple implied volatility surface constructions. Under both specifications, the whole implied volatility surface becomes a solution to a quadratic equation, thus avoiding the numerical issues and computational burdens in numerical integrations, Fourier inversions, nonlinear minimizations associated with existing option pricing models with stochastic volatilities. As a result, constructing implied volatility surfaces based on our models can be 100 times faster than doing so with traditional models. Our extensive calibration exercise on both currency options and equity index options further shows that our lognormal implied variance dynamics specification performs better than traditional stochastic volatility models of similar complexities.

As our approach is quite new, many open questions remain for future research. For example, we derive a fundamental partial differential equation that guarantees dynamic no-arbitrage between any option and a basis option under a single-factor continuous implied volatility dynamics. It remains open on how to guarantee static no-arbitrage among many options across different strikes and maturities. More research is also dearly needed on how to link the implied volatility dynamics to the instantaneous variance rate dynamics, and how to incorporate multiple volatility and return factors as well as discontinuous movements in the price and implied volatility dynamics while retaining simplicity and tractability.

References

Arslan, M., G. Eid, J. E. Khoury, and J. Roth, 2009, “The Gamma Vanna Volga Cost Framework for Constructing Implied Volatility Curves,” manuscript, Deutsche Bank.

Avellaneda, M., and Y. Zhu, 1998, “A Risk-Neutral Stochastic Volatility Model,” *International Journal of Theoretical and Applied Finance*, 1(2), 289–310.

Backus, D., S. Foresi, and L. Wu, 1997, “Accounting for Biases in Black-Scholes,” working paper, New York University.

Bakshi, G., C. Cao, and Z. Chen, 1997, “Empirical Performance of Alternative Option Pricing Models,” *Journal of Finance*, 52(5), 2003–2049.

Bakshi, G., P. Carr, and L. Wu, 2008, “Stochastic Risk Premiums, Stochastic Skewness in Currency Options, and Stochastic Discount Factors in International Economies,” *Journal of Financial Economics*, 87(1), 132–156.

Barndorff-Nielsen, O. E., 1998, “Processes of Normal Inverse Gaussian Type,” *Finance and Stochastics*, 2, 41–68.

Bates, D., 1996, “Jumps and Stochastic Volatility: Exchange Rate Processes Implicit in Deutsche Mark Options,” *Review of Financial Studies*, 9(1), 69–107.

Black, F., and M. Scholes, 1973, “The Pricing of Options and Corporate Liabilities,” *Journal of Political Economy*, 81(3), 637–654.

Carr, P., H. Geman, D. Madan, and M. Yor, 2002, “The Fine Structure of Asset Returns: An Empirical Investigation,” *Journal of Business*, 75(2), 305–332.

Carr, P., and L. Wu, 2003, “Finite Moment Log Stable Process and Option Pricing,” *Journal of Finance*, 58(2), 753–777.

Carr, P., and L. Wu, 2004, "Time-Changed Lévy Processes and Option Pricing," *Journal of Financial Economics*, 71(1), 113–141.

Carr, P., and L. Wu, 2007, "Stochastic Skew in Currency Options," *Journal of Financial Economics*, 86(1), 213–247.

Carr, P., and L. Wu, 2008, "Leverage Effect, Volatility Feedback, and Self-Exciting Market Disruptions: Disentangling the Multi-dimensional Variations in S&P 500 Index Options," working paper, Bloomberg and Baruch College.

Carr, P., and L. Wu, 2010, "Stock Options and Credit Default Swaps: A Joint Framework for Valuation and Estimation," *Journal of Financial Econometrics*, forthcoming.

Castagna, A., and F. Mercurio, 2007, "The Vanna-Volga Method for Implied Volatilities," *Risk*, January, 106–111.

Cox, J. C., and S. A. Ross, 1976, "The Valuation of Options for Alternative Stochastic Processes," *Journal of Financial Economics*, 3(1/2), 145–166.

Daglish, T., J. Hull, and W. Suo, 2007, "Volatility Surfaces: Theory, Rules of Thumb, and Empirical Evidence," *Quantitative Finance*, 7(5), 507–524.

Eberlein, E., U. Keller, and K. Prause, 1998, "New Insights into Smile, Mispricing, and Value at Risk: The Hyperbolic Model," *Journal of Business*, 71(3), 371–406.

Fengler, M. R., 2005, *Semiparametric Modeling of Implied Volatility*. Springer-Verlag, Berlin.

Foresi, S., and L. Wu, 2005, "Crash-O-Phobia: A Domestic Fear or A Worldwide Concern?," *Journal of Derivatives*, 13(2), 8–21.

Gatheral, J., 2006, *The Volatility Surface: A Practitioner's Guide*. John Wiley & Sons, New Jersey.

Hafner, R., 2004, *Stochastic Implied Volatility: A Factor-Based Model*. Springer-Verlag, Berlin.

Harrison, J. M., and D. M. Kreps, 1979, "Martingales and Arbitrage in Multiperiod Securities Markets," *Journal of Economic Theory*, 20(3), 381–408.

Harrison, J. M., and S. R. Pliska, 1981, "Martingales and Stochastic Integrals in the Theory of Continuous Trading," *Stochastic Processes and Their Applications*, 11(3), 215–260.

Heston, S., 1993, "Closed-Form Solution for Options with Stochastic Volatility, with Application to Bond and Currency Options," *Review of Financial Studies*, 6(2), 327–343.

Hodges, H. M., 1996, "Arbitrage Bounds of the Implied Volatility Strike and Term Structures of European-Style Options," *Journal of Derivatives*, 3(4), 23–32.

Huang, J., and L. Wu, 2004, "Specification Analysis of Option Pricing Models Based on Time-Changed Lévy Processes," *Journal of Finance*, 59(3), 1405–1440.

Hull, J., and A. White, 1987, "The Pricing of Options on Assets with Stochastic Volatilities," *Journal of Finance*, 42, 281–300.

Julier, S. J., and J. K. Uhlmann, 1997, "A New Extension of the Kalman filter to Nonlinear Systems," in *Proceedings of AeroSense: The 11th International Symposium on Aerospace/Defense Sensing, Simulation and Controls*, Orlando, Florida.

Kalman, R. E., 1960, "A New Approach to Linear Filtering and Prediction Problems," *Transactions of the ASME–Journal of Basic Engineering*, 82(Series D), 35–45.

Kou, S. G., 2002, "A Jump-Diffusion Model for Option Pricing," *Management Science*, 48(8), 1086–1101.

Ledoit, O., and P. Santa-Clara, 1998, "Relative Pricing of Options with Stochastic Volatility," manuscript, UCLA.

Lee, R., 2004, “The Moment Formula for Implied Volatility at Extreme Strikes,” *Mathematical Finance*, 14(3), 469–480.

Madan, D. B., P. P. Carr, and E. C. Chang, 1998, “The Variance Gamma Process and Option Pricing,” *European Finance Review*, 2(1), 79–105.

Merton, R. C., 1973, “An Intertemporal Asset Pricing Model,” *Econometrica*, 41, 867–887.

Merton, R. C., 1976, “Option Pricing When Underlying Stock Returns Are Discontinuous,” *Journal of Financial Economics*, 3(1), 125–144.

Rogers, L., and M. R. Tehranchi, 2010, “Can the Implied Volatility Surface Move by Parallel Shifts?,” *Finance and Stochastics*, 14(2), 235–248.

Schönbucher, P., 1999, “A Market Model for Stochastic Implied Volatility,” manuscript, ETH Zurich.

Schoutens, W., 2003, *Lévy Processes in Finance: Pricing Financial Derivatives*. John Wiley & Sons Ltd, London.

Wan, E. A., and R. van der Merwe, 2001, “The Unscented Kalman Filter,” in *Kalman Filtering and Neural Networks*, ed. by S. Haykin. Wiley & Sons Publishing, New York, chap. 7, pp. 221–280.

Wu, L., 2006, “Dampened Power Law: Reconciling the Tail Behavior of Financial Asset Returns,” *Journal of Business*, 79(4), 1445–1474.

Wystup, U., 2008, “Vanna Volga Pricing,” manuscript, MathFinance AG.

Table 1

Summary statistics of currency option implied volatility quotes

Entries report the sample average, standard deviation, and weekly autocorrelation of the implied volatility quotes on the dollar price of yen (JPYUSD) and the dollar price of pound (GBPUSD). Data are weekly from January 8, 1997 to December 26, 2007, 573 observations for each series for 55 series, including five deltas at each maturity at 10-delta put (10p), 25-delta put (25p), delta-neutral straddle (S), 25-delta call (25c), and 10-delta call (10c), and 11 maturities from one to 60 months.

Currency	JPYUSD					GBPUSD				
Delta	10p	25p	S	25c	10c	10p	25p	S	25c	10c
Mat	A. Sample Average									
1	11.09	10.67	10.79	11.58	12.79	8.98	8.50	8.28	8.45	8.89
2	11.07	10.59	10.68	11.44	12.66	9.02	8.54	8.32	8.51	8.96
3	11.18	10.63	10.71	11.47	12.73	9.14	8.63	8.42	8.62	9.10
6	11.38	10.72	10.77	11.55	12.92	9.25	8.74	8.53	8.74	9.25
9	11.44	10.75	10.80	11.59	13.03	9.31	8.79	8.58	8.79	9.32
12	11.49	10.78	10.83	11.63	13.12	9.34	8.82	8.61	8.83	9.36
18	11.44	10.74	10.84	11.69	13.27	9.41	8.90	8.70	8.91	9.43
24	10.99	10.60	10.85	11.59	12.91	9.21	8.87	8.77	8.90	9.26
36	10.66	10.46	10.91	11.77	13.12	9.25	8.98	8.89	8.99	9.28
48	10.65	10.53	11.06	11.97	13.43	9.32	9.08	9.01	9.09	9.34
60	10.75	10.69	11.28	12.21	13.78	9.42	9.19	9.12	9.20	9.43
	B. Standard Deviation									
1	3.08	2.96	2.97	3.25	3.75	1.48	1.39	1.33	1.33	1.39
2	3.16	2.93	2.82	2.97	3.35	1.35	1.26	1.21	1.22	1.27
3	3.24	2.95	2.74	2.80	3.11	1.28	1.19	1.14	1.15	1.18
6	3.42	3.05	2.74	2.67	2.88	1.17	1.09	1.05	1.05	1.07
9	3.48	3.10	2.75	2.64	2.82	1.13	1.05	1.01	1.01	1.02
12	3.53	3.14	2.77	2.63	2.80	1.10	1.03	0.99	0.98	0.98
18	3.52	3.16	2.78	2.59	2.71	1.08	1.02	0.99	0.97	0.96
24	2.95	3.01	2.79	2.38	2.11	1.06	1.00	0.99	0.96	0.97
36	3.05	3.12	2.80	2.29	2.03	0.99	0.99	1.00	0.97	0.93
48	3.10	3.15	2.77	2.20	1.98	0.98	1.00	1.03	0.99	0.93
60	3.11	3.15	2.73	2.13	1.96	0.97	1.02	1.05	1.01	0.93
	C. Weekly Autocorrelation									
1	0.94	0.94	0.93	0.93	0.93	0.91	0.91	0.90	0.90	0.90
2	0.96	0.96	0.95	0.95	0.94	0.94	0.93	0.93	0.93	0.93
3	0.98	0.97	0.97	0.96	0.96	0.95	0.94	0.94	0.94	0.94
6	0.99	0.99	0.98	0.98	0.97	0.96	0.96	0.96	0.96	0.96
9	0.99	0.99	0.99	0.98	0.98	0.97	0.97	0.97	0.97	0.96
12	0.99	0.99	0.99	0.98	0.98	0.97	0.97	0.97	0.97	0.97
18	0.99	0.99	0.99	0.98	0.98	0.97	0.97	0.97	0.97	0.97
24	0.99	0.99	0.99	0.98	0.96	0.97	0.97	0.97	0.97	0.97
36	0.99	0.99	0.99	0.98	0.96	0.97	0.97	0.97	0.97	0.97
48	0.99	0.99	0.99	0.98	0.96	0.97	0.97	0.97	0.97	0.97
60	0.99	0.99	0.99	0.98	0.96	0.96	0.97	0.97	0.97	0.97

Table 2

Summary statistics of pricing errors on dollar-yen option implied volatilities

Entries report the summary statistics of the pricing errors on dollar-yen option implied volatilities in percentage points. The explained variation is defined as one minus the ratio of the pricing error variance to the variance of the implied volatility observation.

Model	SRV					LNV					Heston				
Delta	10p	25p	S	25c	10c	10p	25p	S	25c	10c	10p	25p	S	25c	10c
A. Root Mean Squared Error															
1	0.66	0.53	0.55	0.61	1.03	0.65	0.52	0.53	0.55	0.76	0.78	0.48	0.43	0.42	0.83
2	0.42	0.33	0.37	0.32	0.51	0.41	0.33	0.36	0.27	0.36	0.47	0.28	0.28	0.26	0.38
3	0.29	0.25	0.29	0.23	0.43	0.30	0.24	0.26	0.16	0.35	0.31	0.19	0.23	0.22	0.30
6	0.41	0.30	0.31	0.31	0.37	0.32	0.32	0.28	0.22	0.37	0.39	0.30	0.27	0.24	0.34
9	0.55	0.26	0.26	0.33	0.35	0.44	0.33	0.25	0.22	0.31	0.52	0.34	0.26	0.24	0.39
12	0.65	0.27	0.24	0.33	0.46	0.55	0.33	0.23	0.22	0.37	0.61	0.37	0.25	0.24	0.44
18	0.65	0.26	0.20	0.30	0.62	0.61	0.27	0.18	0.18	0.55	0.62	0.30	0.19	0.20	0.48
24	0.34	0.29	0.19	0.36	0.49	0.30	0.25	0.16	0.25	0.45	0.33	0.18	0.18	0.29	0.53
36	0.59	0.35	0.19	0.27	0.28	0.49	0.37	0.16	0.31	0.27	0.46	0.33	0.17	0.27	0.45
48	0.65	0.29	0.23	0.30	0.41	0.53	0.34	0.25	0.48	0.24	0.53	0.34	0.19	0.31	0.51
60	0.59	0.29	0.42	0.49	0.77	0.47	0.31	0.49	0.71	0.44	0.52	0.36	0.37	0.47	0.71
Average:			**0.40**					**0.36**					**0.37**		
B. Explained Variation															
1	0.95	0.98	0.97	0.97	0.95	0.96	0.98	0.97	0.97	0.97	0.94	0.98	0.98	0.98	0.97
2	0.98	0.99	0.99	0.99	0.98	0.98	0.99	0.99	0.99	0.99	0.98	0.99	0.99	0.99	0.99
3	0.99	0.99	0.99	1.00	0.98	0.99	1.00	0.99	1.00	0.99	0.99	1.00	0.99	0.99	0.99
6	0.99	0.99	0.99	0.99	0.98	0.99	0.99	0.99	0.99	0.99	0.99	0.99	0.99	0.99	0.99
9	0.98	0.99	0.99	0.99	0.98	0.99	0.99	0.99	0.99	0.99	0.99	0.99	0.99	0.99	0.98
12	0.98	0.99	0.99	0.99	0.97	0.98	0.99	0.99	0.99	0.98	0.98	0.99	0.99	0.99	0.98
18	0.98	0.99	1.00	0.99	0.95	0.98	0.99	1.00	1.00	0.96	0.98	0.99	1.00	0.99	0.97
24	0.99	0.99	1.00	0.99	0.96	0.99	1.00	1.00	0.99	0.97	0.99	1.00	1.00	0.99	0.96
36	0.98	0.99	1.00	0.99	0.98	0.99	1.00	1.00	0.98	0.99	0.99	0.99	1.00	0.99	0.96
48	0.98	0.99	0.99	0.98	0.97	0.98	1.00	0.99	0.97	0.99	0.98	0.99	1.00	0.98	0.93
60	0.98	0.99	0.98	0.96	0.91	0.98	0.99	0.98	0.95	0.96	0.98	0.99	0.99	0.96	0.89
Average:			**0.98**					**0.99**					**0.98**		
C. Weekly Error Autocorrelation															
1	0.83	0.64	0.58	0.65	0.73	0.84	0.62	0.52	0.60	0.71	0.90	0.76	0.69	0.64	0.75
2	0.84	0.52	0.48	0.48	0.71	0.85	0.40	0.31	0.38	0.75	0.87	0.58	0.65	0.56	0.72
3	0.84	0.78	0.80	0.61	0.88	0.85	0.67	0.63	0.46	0.89	0.81	0.66	0.82	0.71	0.75
6	0.85	0.85	0.86	0.81	0.83	0.78	0.88	0.84	0.75	0.86	0.87	0.88	0.89	0.84	0.86
9	0.91	0.81	0.83	0.83	0.81	0.87	0.88	0.80	0.75	0.81	0.93	0.91	0.88	0.86	0.91
12	0.93	0.80	0.80	0.83	0.88	0.92	0.88	0.77	0.76	0.88	0.95	0.92	0.86	0.85	0.93
18	0.95	0.82	0.77	0.86	0.95	0.95	0.89	0.75	0.76	0.95	0.97	0.94	0.89	0.86	0.95
24	0.86	0.86	0.74	0.86	0.90	0.86	0.79	0.74	0.88	0.88	0.89	0.86	0.91	0.88	0.92
36	0.91	0.87	0.68	0.83	0.82	0.91	0.82	0.72	0.90	0.72	0.90	0.90	0.88	0.91	0.92
48	0.91	0.78	0.71	0.86	0.87	0.90	0.77	0.81	0.92	0.76	0.92	0.87	0.85	0.93	0.94
60	0.88	0.76	0.85	0.91	0.92	0.87	0.82	0.90	0.94	0.87	0.92	0.89	0.93	0.96	0.96
Average:			**0.80**					**0.78**					**0.85**		

Table 3

Summary statistics of pricing errors on dollar-pound option implied volatilities

Entries report the summary statistics of the pricing errors on over-the-counter dollar-pound option implied volatilities in percentage points. The explained variation is defined as one minus the ratio of the pricing error variance to the variance of the implied volatility observation.

Model	SRV					LNV					Heston				
Delta	10p	25p	S	25c	10c	10p	25p	S	25c	10c	10p	25p	S	25c	10c
A. Root Mean Squared Error															
1	0.24	0.17	0.18	0.15	0.25	0.22	0.16	0.18	0.14	0.24	0.26	0.16	0.15	0.16	0.26
2	0.13	0.12	0.14	0.11	0.12	0.12	0.11	0.14	0.10	0.11	0.14	0.10	0.10	0.10	0.14
3	0.11	0.10	0.10	0.09	0.12	0.11	0.09	0.09	0.09	0.11	0.12	0.10	0.13	0.09	0.12
6	0.12	0.09	0.08	0.09	0.14	0.12	0.09	0.07	0.08	0.13	0.12	0.09	0.13	0.09	0.12
9	0.15	0.09	0.08	0.09	0.15	0.14	0.10	0.08	0.09	0.14	0.14	0.09	0.11	0.09	0.13
12	0.19	0.11	0.09	0.11	0.16	0.16	0.11	0.09	0.10	0.15	0.15	0.10	0.13	0.10	0.15
18	0.22	0.10	0.08	0.08	0.15	0.19	0.11	0.08	0.08	0.14	0.18	0.09	0.12	0.09	0.18
24	0.26	0.12	0.08	0.10	0.23	0.24	0.12	0.08	0.10	0.21	0.25	0.14	0.12	0.12	0.19
36	0.14	0.07	0.05	0.07	0.15	0.13	0.08	0.05	0.07	0.14	0.17	0.09	0.11	0.09	0.13
48	0.14	0.09	0.08	0.09	0.15	0.13	0.09	0.08	0.09	0.13	0.17	0.11	0.13	0.11	0.14
60	0.22	0.16	0.15	0.16	0.22	0.22	0.16	0.15	0.16	0.21	0.24	0.19	0.20	0.18	0.21
Average:			**0.13**					**0.12**					**0.14**		
B. Explained Variation															
1	0.98	0.99	0.99	0.99	0.98	0.98	0.99	0.99	0.99	0.98	0.98	0.99	0.99	0.99	0.97
2	0.99	0.99	0.99	0.99	0.99	0.99	0.99	0.99	0.99	0.99	0.99	0.99	0.99	0.99	0.99
3	0.99	0.99	0.99	0.99	0.99	0.99	0.99	0.99	0.99	0.99	0.99	0.99	0.99	0.99	0.99
6	0.99	0.99	0.99	0.99	0.98	0.99	0.99	0.99	0.99	0.99	0.99	0.99	0.99	0.99	0.99
9	0.98	0.99	0.99	0.99	0.98	0.99	0.99	0.99	0.99	0.98	0.99	0.99	0.99	0.99	0.98
12	0.97	0.99	0.99	0.99	0.98	0.98	0.99	0.99	0.99	0.98	0.98	0.99	0.99	0.99	0.98
18	0.96	0.99	0.99	0.99	0.97	0.97	0.99	0.99	0.99	0.98	0.98	0.99	0.99	0.99	0.97
24	0.95	0.99	1.00	0.99	0.97	0.96	0.99	1.00	0.99	0.97	0.95	0.99	1.00	0.99	0.97
36	0.98	1.00	1.00	1.00	0.98	0.98	0.99	1.00	1.00	0.99	0.97	1.00	1.00	1.00	0.98
48	0.98	0.99	0.99	0.99	0.98	0.99	0.99	0.99	0.99	0.98	0.97	0.99	0.98	0.99	0.98
60	0.97	0.99	0.98	0.98	0.96	0.98	0.99	0.98	0.98	0.97	0.96	0.97	0.97	0.97	0.98
Average:			**0.99**					**0.99**					**0.98**		
C. Weekly Error Autocorrelation															
1	0.62	0.51	0.48	0.46	0.67	0.69	0.51	0.47	0.47	0.71	0.70	0.57	0.57	0.59	0.76
2	0.56	0.49	0.55	0.49	0.54	0.63	0.48	0.53	0.49	0.56	0.60	0.54	0.59	0.55	0.60
3	0.53	0.46	0.52	0.42	0.62	0.60	0.43	0.50	0.44	0.64	0.55	0.48	0.50	0.46	0.57
6	0.75	0.64	0.58	0.59	0.77	0.74	0.66	0.59	0.61	0.76	0.79	0.65	0.76	0.65	0.78
9	0.86	0.70	0.62	0.66	0.81	0.85	0.75	0.66	0.68	0.80	0.87	0.76	0.85	0.75	0.85
12	0.90	0.77	0.71	0.74	0.84	0.90	0.81	0.74	0.76	0.84	0.90	0.82	0.86	0.80	0.87
18	0.95	0.85	0.79	0.79	0.91	0.95	0.87	0.78	0.81	0.91	0.94	0.86	0.86	0.84	0.93
24	0.94	0.89	0.81	0.85	0.95	0.95	0.90	0.80	0.86	0.94	0.95	0.87	0.86	0.84	0.94
36	0.91	0.83	0.70	0.82	0.92	0.91	0.86	0.69	0.84	0.92	0.94	0.80	0.87	0.80	0.91
48	0.89	0.83	0.86	0.87	0.91	0.90	0.84	0.85	0.86	0.92	0.93	0.90	0.93	0.88	0.88
60	0.84	0.78	0.83	0.82	0.87	0.84	0.77	0.83	0.81	0.87	0.88	0.87	0.90	0.85	0.79
Average:			**0.73**					**0.74**					**0.78**		

Table 4

Summary statistics of over-the-counter S&P 500 index option implied volatility quotes

Entries report the sample average, standard deviation, and weekly autocorrelation of 40 over-the-counter implied volatility quotes on the S&P 500 index options across five relative strikes (K/S) and eight time to maturities (in months). The data are weekly from January 8, 1997 to December 26, 2007, 573 observations for each series.

K/S	0.8	0.9	1.0	1.1	1.2
Mat			A. Sample Average		
1	33.75	25.81	18.71	15.06	14.26
3	28.86	23.88	19.31	15.97	14.56
6	26.61	23.04	19.68	16.90	15.21
12	25.12	22.57	20.14	17.97	16.32
24	24.49	22.65	20.89	19.24	17.82
36	24.41	22.93	21.50	20.16	18.93
48	24.52	23.25	22.04	20.90	19.83
60	24.72	23.60	22.55	21.55	20.60
			B. Standard Deviation		
1	6.68	6.22	6.06	5.11	4.55
3	5.92	5.62	5.42	4.94	4.27
6	5.27	5.08	4.93	4.73	4.22
12	4.82	4.68	4.59	4.49	4.20
24	4.65	4.51	4.39	4.31	4.15
36	4.43	4.35	4.28	4.23	4.14
48	4.23	4.19	4.16	4.14	4.10
60	4.10	4.08	4.06	4.04	4.03
			C. Weekly Autocorrelation		
1	0.94	0.94	0.94	0.95	0.96
3	0.97	0.96	0.96	0.96	0.97
6	0.97	0.97	0.97	0.97	0.97
12	0.98	0.98	0.98	0.98	0.98
24	0.99	0.99	0.99	0.99	0.98
36	0.99	0.99	0.99	0.99	0.99
48	0.99	0.99	0.99	0.99	0.99
60	0.99	0.99	0.99	0.99	0.99

Table 5

Summary statistics of pricing errors on S&P 500 index option implied volatilities

Entries report the summary statistics of the pricing errors on S&P 500 index option implied volatilities in percentage points. The explained variation is defined as one minus the ratio of the pricing error variance to the variance of the implied volatility observation.

Model	SRV					LNV					Heston				
K/S	0.8	0.9	1.0	1.1	1.2	0.8	0.9	1.0	1.1	1.2	0.8	0.9	1.0	1.1	1.2
A. Root Mean Squared Error															
1	4.74	0.95	2.14	1.01	0.79	2.14	1.01	1.16	0.80	0.97	5.10	2.42	1.65	2.05	2.98
3	0.88	1.25	1.06	0.84	0.57	1.36	0.44	0.37	0.40	0.42	1.93	1.03	1.13	1.90	1.51
6	1.48	1.16	0.56	0.77	0.61	1.80	0.47	0.46	0.38	0.48	1.25	0.88	1.10	1.95	1.64
12	1.21	0.66	0.42	0.60	0.66	1.23	0.34	0.67	0.46	0.53	0.95	0.68	0.78	1.26	1.65
24	0.59	0.51	0.45	0.34	0.77	0.38	0.61	0.68	0.35	0.64	0.78	0.50	0.41	0.59	0.97
36	0.73	0.58	0.35	0.29	0.90	0.48	0.65	0.52	0.22	0.74	0.61	0.38	0.30	0.43	0.68
48	0.97	0.64	0.27	0.35	0.98	0.62	0.57	0.33	0.29	0.90	0.56	0.39	0.32	0.40	0.59
60	1.23	0.79	0.36	0.40	0.99	0.72	0.51	0.24	0.47	1.05	0.72	0.60	0.52	0.53	0.62
Average:			**0.87**					**0.67**					**1.12**		
B. Explained Variation															
1	0.91	0.98	0.97	0.99	0.97	0.98	0.99	0.98	0.98	0.97	0.83	0.90	0.93	0.84	0.67
3	0.98	0.99	0.99	0.99	0.99	0.99	1.00	1.00	0.99	0.99	0.93	0.97	0.97	0.91	0.88
6	0.98	0.99	0.99	1.00	0.98	0.98	0.99	1.00	1.00	0.99	0.94	0.97	0.98	0.93	0.88
12	0.98	0.99	0.99	0.99	0.98	0.99	1.00	1.00	1.00	0.99	0.96	0.98	0.99	0.97	0.90
24	0.98	0.99	1.00	0.99	0.99	0.99	1.00	1.00	1.00	0.99	0.97	0.99	0.99	0.98	0.95
36	0.99	0.99	1.00	1.00	0.99	0.99	1.00	1.00	1.00	1.00	0.98	0.99	1.00	0.99	0.97
48	0.98	1.00	1.00	1.00	0.99	0.99	1.00	1.00	1.00	1.00	0.98	0.99	0.99	0.99	0.98
60	0.97	0.99	1.00	1.00	0.99	0.99	1.00	1.00	1.00	0.99	0.98	0.99	0.99	0.98	0.98
Average:			**0.99**					**0.99**					**0.95**		
C. Weekly Error Autocorrelation															
1	0.89	0.80	0.84	0.82	0.76	0.84	0.69	0.68	0.80	0.73	0.85	0.89	0.84	0.84	0.78
3	0.89	0.83	0.90	0.79	0.62	0.84	0.81	0.71	0.68	0.72	0.94	0.89	0.84	0.84	0.72
6	0.89	0.88	0.88	0.67	0.78	0.87	0.87	0.79	0.69	0.79	0.94	0.91	0.85	0.84	0.79
12	0.84	0.87	0.84	0.78	0.87	0.84	0.79	0.81	0.76	0.79	0.92	0.90	0.85	0.88	0.88
24	0.91	0.92	0.88	0.86	0.90	0.85	0.72	0.79	0.78	0.80	0.91	0.85	0.77	0.86	0.91
36	0.91	0.89	0.82	0.85	0.88	0.83	0.66	0.72	0.72	0.73	0.86	0.75	0.66	0.82	0.89
48	0.94	0.86	0.60	0.82	0.90	0.88	0.64	0.59	0.73	0.81	0.85	0.76	0.73	0.82	0.89
60	0.96	0.92	0.83	0.83	0.89	0.92	0.76	0.65	0.77	0.86	0.89	0.87	0.87	0.89	0.91
Average:			**0.84**					**0.77**					**0.85**		

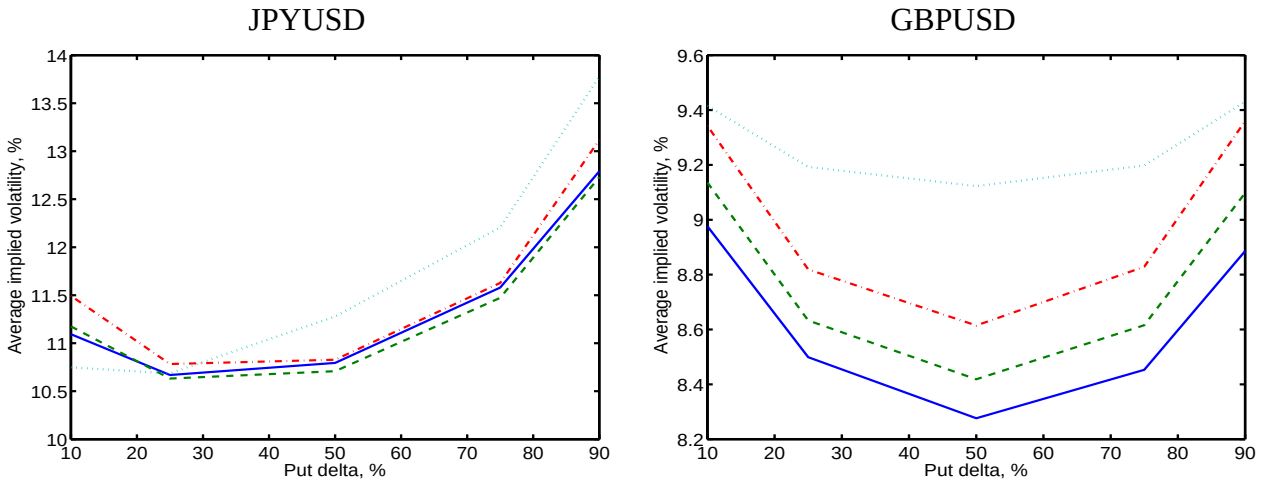

Figure 1

Average implied volatility smiles on currency options

Lines plot the time-series average of the implied volatility quotes in percentage points against the put delta of the currency options at four selected maturities: one month (solid lines), three months (dashed lines), one year (dashdotted lines), and five years (dotted lines). The averages are on weekly data from January 8, 1997, to December 26, 2007, 573 observations for each series. 10- and 25-delta call implied volatilities are approximated as implied volatilities for 90- and 75-delta puts.

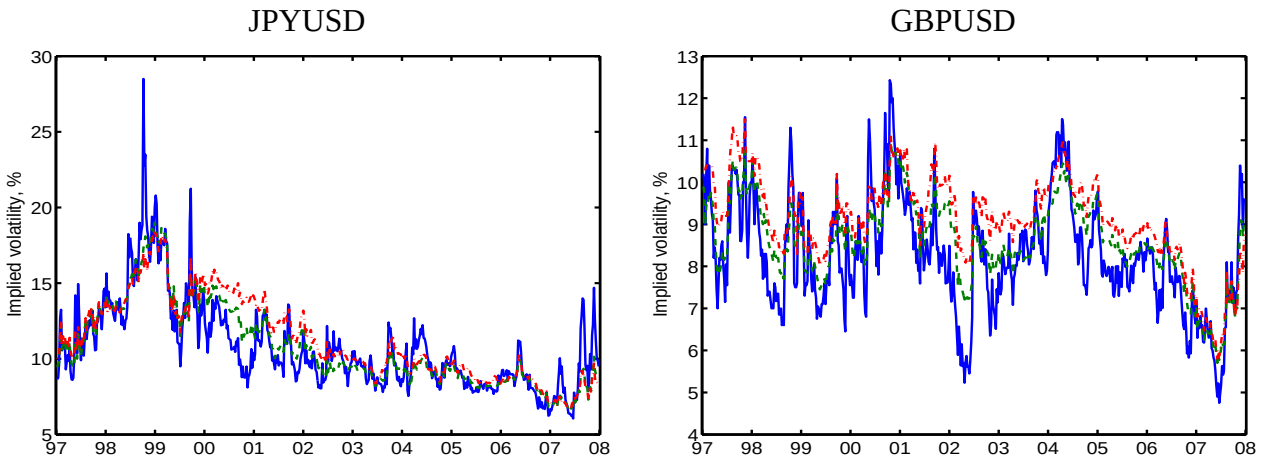

Figure 2

The time series of delta-neutral straddle implied volatilities

Lines plot the time-series of the delta-neutral straddle implied volatilities at three selected maturities: one month (solid lines), three months (dashed lines), and five years (dashdotted lines).

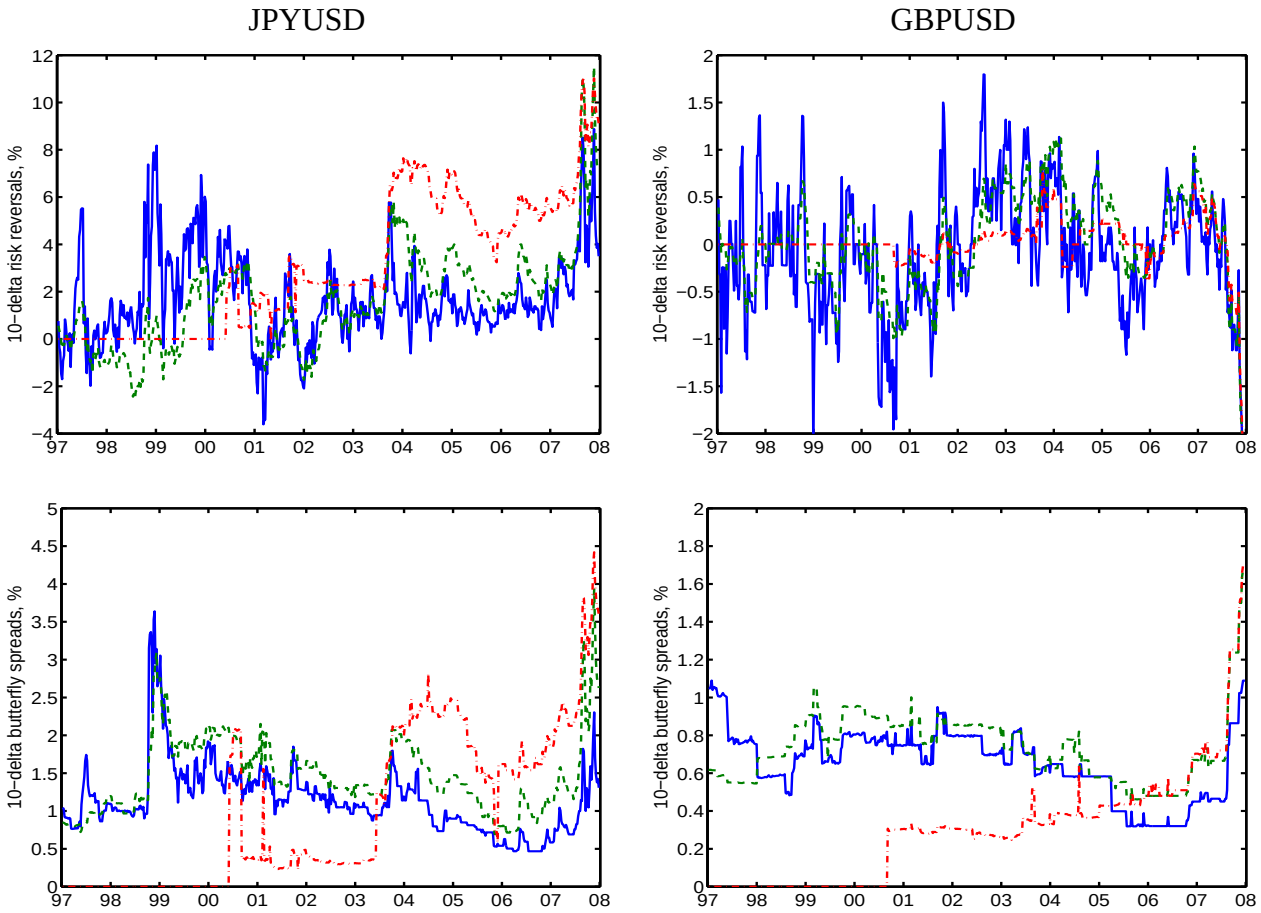

Figure 3
The time series of 10-delta risk reversals and butterfly spreads
Lines plot the time-series of the 10-delta risk reversals in the top two panels and 10-delta butterfly spreads in the bottom two panel. Each panel is for one currency pair. The three lines in each panel represent three selected maturities at one month (solid lines), three months (dashed lines), and five years (dashdotted lines).

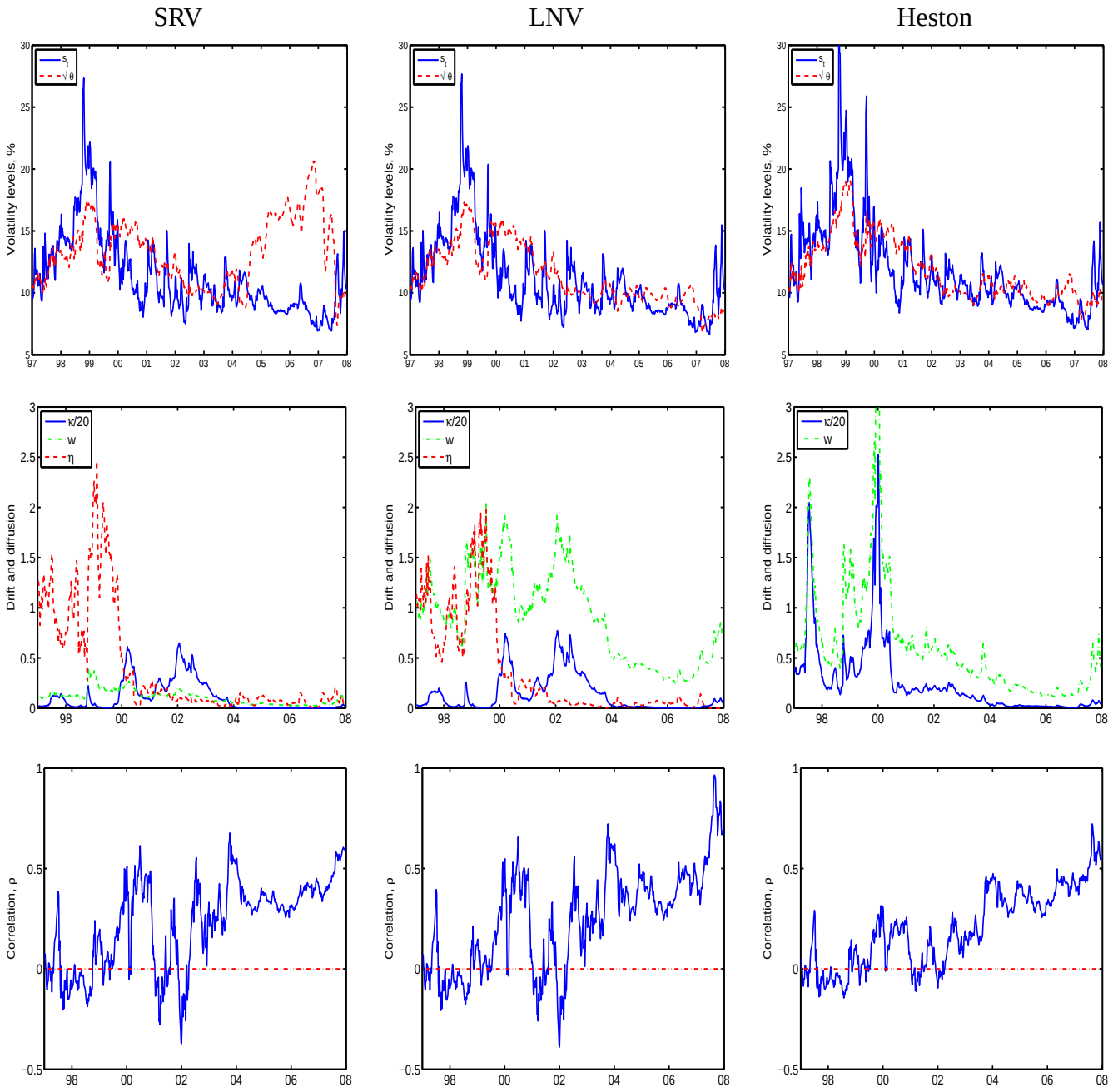

Figure 4

Time-varying coefficients calibrated to dollar-yen option implied volatilities

The nine panels plot the time series of model coefficients calibrated to the dollar-yen options under the SRV model (left), the LNV model (middle), and the Heston model (right). The coefficients for each model are grouped into three panels.

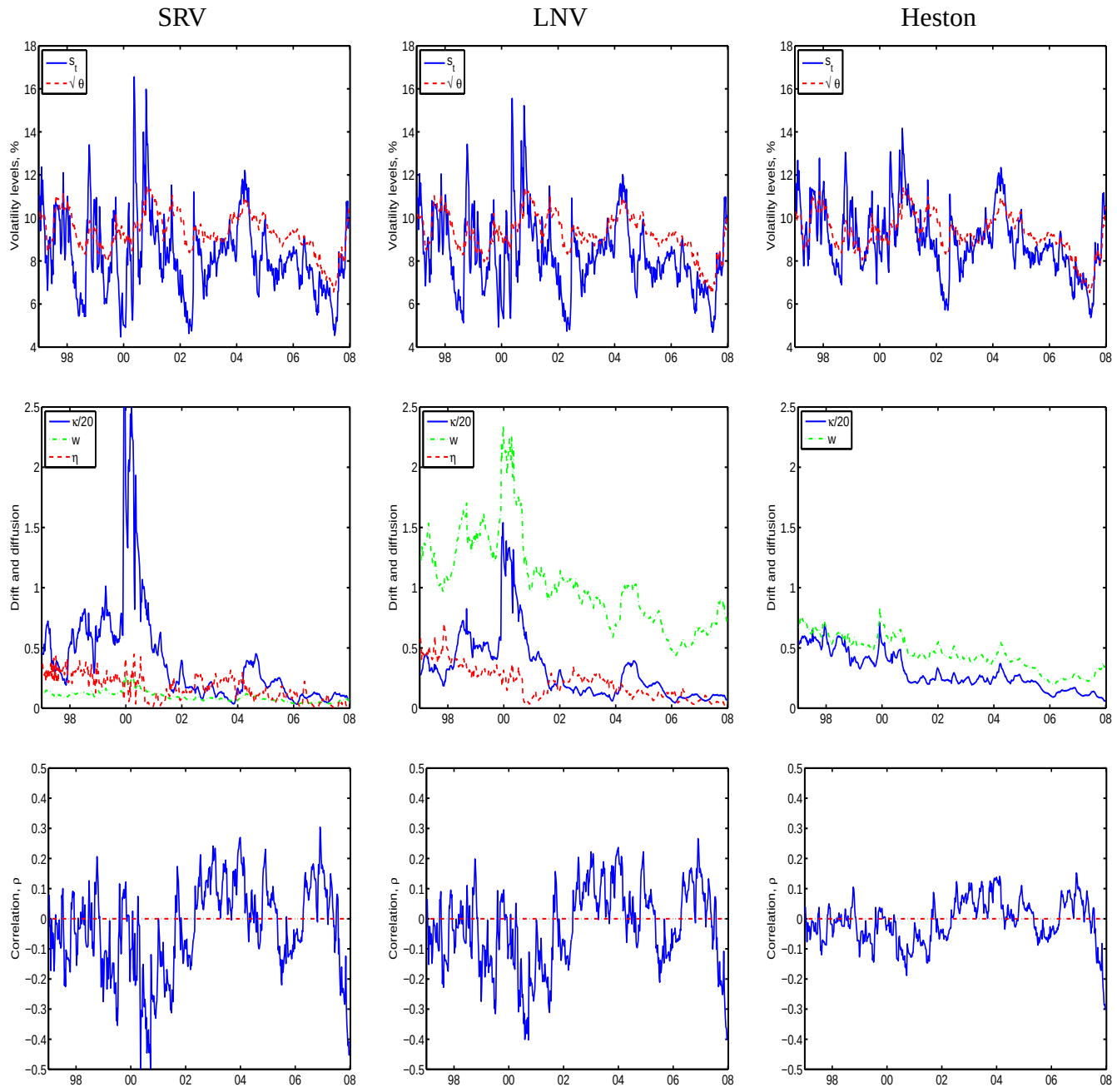

Figure 5

Time-varying coefficients calibrated to dollar-pound option implied volatilities

The nine panels plot the time series of model coefficients calibrated to the dollar-pound options under the SRV model (left), the LNV model (middle), and the Heston model (right). The coefficients for each model are grouped into three panels.

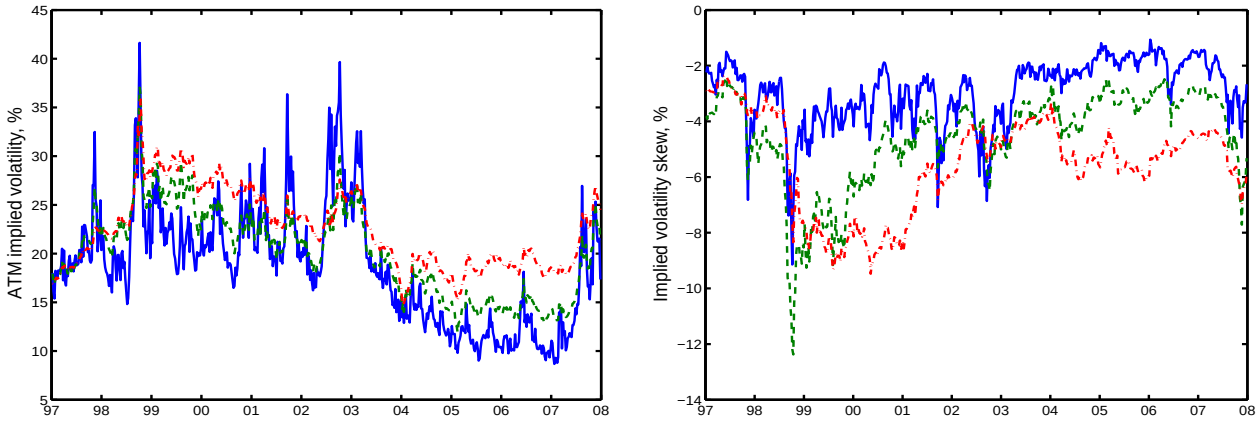

Figure 6

The time series of at-the-money implied volatilities and skews on SPX options

Lines denote the time series of the SPX option at-the-money implied volatilities in the left panel and the implied volatility skew in the right panel. The three lines in each panel represent three maturities at one month (solid line), one year (dashed line), and five years (dash-dotted line). The implied volatility skew is defined as the percentage volatility point difference between 80% and 120% strike implied volatilities scaled by the corresponding difference in the standardized moneyness measure *z*.

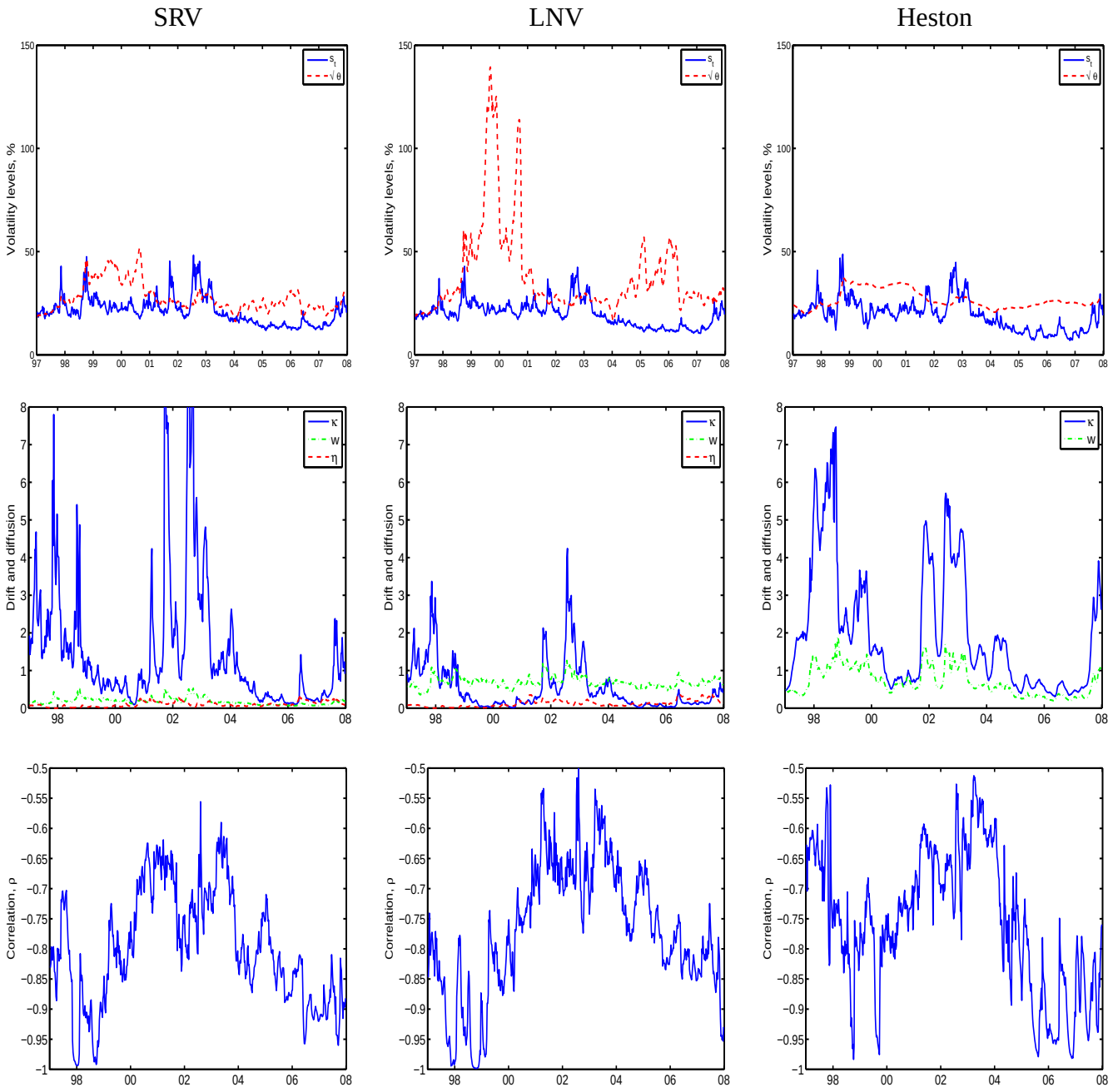

Figure 7

Time-varying coefficients calibrated to SPX option implied volatilities

The nine panels plot the time series of model coefficients calibrated to the SPX index option implied volatilities under the SRV model (left), the LNV model (middle), and the Heston model (right). The coefficients for each model are grouped into three panels.